RADIATIVE DECAYS IN THE ψ FAMILY

Kay KÖNIGSMANN

Universität Würzburg, 8700 *Würzburg*, *Fed. Rep. Germany*

and

Deutsches Elektronen-Synchrotron DESY, 2000 *Hamburg*, *Fed. Rep. Germany*

NORTH-HOLLAND – AMSTERDAM

PHYSICS REPORTS (Review Section of Physics Letters) 139, No. 5 (1986) 243–291. North-Holland, Amsterdam

RADIATIVE DECAYS IN THE ψ FAMILY

Kay KÖNIGSMANN

Universität Würzburg, 8700 Würzburg, Fed. Rep. Germany

and

Deutsches Elektronen-Synchrotron DESY, 2000 Hamburg, Fed. Rep. Germany

Received 13 January 1986

Contents

Abstract:

This report presents a summary on radiative decays of the ψ states. Most of the experimental information has been obtained by the experiments DM2, Mark III and Crystal Ball, operating at the storage rings DCI and SPEAR. Radiative decays from the ψ′ yields an abundance of information on the *C*-parity even states within the charmonium system. Nearly all experimental data on χ and η_c mesons compare favorably with theoretical predictions. Overall, an impressive agreement emerges between charmonium spectroscopy and theoretical models. Radiative transitions from J/ψ to light mesons have helped to better understand the low lying nonets. Two unexpected resonances, the ι(1460) and Θ(1700), have large production rates and exhibit unusual decay properties. The Θ is almost certainly a non-$q\bar{q}$ state and qualifies as a gluonic meson candidate. The ι is more controversial. A classification will have to depend on a detailed understanding of the excited pseudoscalar nonet. Finally, evidence for the ξ(2200) will be reported and its interpretation will be reviewed.

Single orders for this issue

PHYSICS REPORTS (Review Section of Physics Letters) 139, No. 5 (1986) 243–291.

Copies of this issue may be obtained at the price given below. All orders should be sent directly to the Publisher. Orders must be accompanied by check.

Single issue price Dfl. 33.00, postage included.

1. Introduction

One of the main concerns of physics in this century has been the quest for the constituents of matter and the laws which govern their behavior. The progressively more detailed understanding of the emission and absorption spectra of atoms has led from Bohr's theory of the hydrogen atom to the postulation of the electron spin and to Pauli's exclusion principle. Ultimately, the formulation of the non-relativistic quantum mechanical Schrödinger equation evolved from the study of atomic spectroscopy. Scattering experiments and spectroscopic investigations of the nucleus and the nucleon have subsequently helped to determine the substructure of those systems. In the current view of particle physics the fundamental constituents of matter are point-like, structureless objects of spin one-half: the quarks and leptons. Quarks undergo the strong, electromagnetic and weak interactions. They are the building blocks of hadrons like the proton and neutron. Leptons – like the electron and muon – on the other hand, do not feel the strong force and interact only via the electromagnetic and weak force.

Three different quarks u, d and s were originally postulated by Gell-Mann and Zweig [1] to account for the structure and properties of hadrons known at that time. Strong evidence for the existence of quarks inside a nucleus was provided by deep inelastic scattering experiments which probed the interior of nuclei at very short distances. However, it was the discovery of the J/ψ [2, 3] and the observation of hadrons containing a fourth quark [4], the charmed c quark, which finally confirmed this view. More recently, evidence for an even heavier b quark was obtained with the discovery of the Υ meson [5]. As free quarks have not yet been seen their properties have to be inferred from the observed properties of hadrons. According to the quark model, hadrons are divided into two categories: baryons, each containing three quarks, and mesons, each containing a quark and an antiquark. Heavy mesons are defined to contain at least one heavy c or b quark. Mesons consisting of two heavy quarks of the same kind are referred to as quarkonium states, in analogy to positronium, which is a bound system of an electron and its antiparticle, the positron.

At present, the Standard Model [6] of high energy physics assumes six varieties (flavor) of quarks and six leptons. The quarks carry charges $\frac{2}{3}e$ and $-\frac{1}{3}e$ and are grouped in three generations: (u, d) (c, s) (t, b). Substantial evidence for the t quark has not yet been accumulated. Like the six leptons (e^-, ν_e) (μ^-, ν_μ) (τ^-, ν_τ), the quarks are spin 1/2 fermions. In addition, quarks carry a new quantum number called color. The non-observation of free quarks is summarized in the requirement of color confinement: no state explicitly carrying color can be observed. By treating color as a strong charge, quantum chromodynamics (QCD) [7] emerges as the theory of the strong interaction of quarks. An octet of massless colored spin 1 bosons, the gluons, mediate the interaction between quarks and are thus responsible for the binding of quarks in hadrons.

Of particular interest for the study of the strong interactions are quarkonia systems. A specific example of such a bound state of a heavy quark and its antiquark is the $c\bar{c}$ charmonium system. This review deals with charmonium states below the open charm threshold, where decays to mesons containing one charmed quark are energetically impossible and the main decay mechanism proceeds by annihilation of the charmed quark and its antiquark into gluons. The $J^{PC} = 1^{--}$ vector states J/ψ and ψ′ can be produced directly in e^+e^- annihilations and provide the basis for a detailed spectroscopic study of energy levels and transition rates. Radiative transitions within the charmonium system reveal the predicted $c\bar{c}$ C-even χ and η_c states and probe the wave function at distances larger than the average radius of the ψ bound system. Radiative as well as hadronic decays to *light* mesons, however, give information on the value of the wave function at the origin. Together with a study of energy levels, which determines the potential at an intermediate distance, a coherent picture of the dynamics of the quark interaction emerges.

The decay of $J^{PC} = 1^{--}$ charmonium states to mesons not containing c quarks proceeds mainly by emission of three gluons which fragment into light hadrons. In addition, the radiative decay into a photon and two gluons constitutes a substantial fraction of the total decay rate. The two-gluon system may form well-known $q\bar{q}$ mesons like η, η', etc. As the intermediate state is rich in gluons, radiative decays are very well suited to search for exotic states with large gluon contents. Due to the non-Abelian nature of the SU(3) color group governing the strong interaction, gluons interact with each other and may form bound states with no quark content, gluonic mesons [8] (also called glueballs or gluonium). On the other hand, hybrid mesons [9] (also termed meiktons) are $q\bar{q}$ mesons with one additional gluon. Note that these states can be called mesons if a meson is defined, independent of its contents, to have integer total spin and zero baryon number. It is not yet completely clear whether QCD really requires these and other exotic states to exist. Radiative decays of charmonium offer the possibility to investigate the spectrum of light mesons and search for new effects expected within or outside the Standard Model.

This report is divided into eight chapters. After the introduction, chapter 2 describes the four detectors which have furnished most of the physics results to be presented here. Radiative transitions to the charmonium χ and η_c states are treated in chapter 3. Results on branching ratios, masses and hadronic widths are compared with QCD model predictions. Chapters 4, 5 and 6 contain results on radiative transitions to light mesons, which are grouped according to the meson spin-parities. The pseudoscalar particles discussed in chapter 4 are the neutral members of the ground state nonet π^0, η and η', and a new resonance, the $\iota(1460)$. Theoretical interpretations for the ι are reviewed in context with the E(1420) meson. The two vector particle final states $\rho\rho$, $\omega\omega$, and $\phi\phi$ are analyzed in chapter 5 with respect to their possible origin from the ι. The tensor mesons f(1270), f'(1525) and another new state, $\Theta(1700)$, are discussed in chapter 6. Whereas the f and f' behave like normal $q\bar{q}$ mesons, the Θ remains unexplainable as a $q\bar{q}$ resonance. Its likely interpretation is a gluonium resonance. Chapter 7 reports the evidence for a heavy, narrow resonance $\xi(2200)$. An explanation of this particle in terms of a high spin $s\bar{s}$ state is fully compatible with experimental data. Also reviewed is the search for the axion, a Goldstone boson predicted in theories of the strong interactions. Finally, radiative decays from the ψ' are compared to those from the J/ψ with the interesting result that radiative transitions from the ψ' to η and η' are suppressed. Chapter 8 summarises the physics of radiative transitions from charmonium states and gives an outlook on what we may expect to learn in the near future.

2. Detectors

Most of the data to be discussed here were obtained by the experiments Crystal Ball [10], DM2 [11], Mark II [12] and Mark III [13]. The DM2 detector has been operating at the DCI storage ring at Orsay. All other three detectors have taken data at the SPEAR storage ring at the Stanford Linear Accelerator Center SLAC. Results based on rather small event samples from the DASP [14], DESY–Heidelberg [15] and PLUTO [16] experiments, which operated at the storage ring DORIS at DESY, are also included.

All three electron–positron colliding machines have been very well suited for a study of the charmonium system in the center-of-mass energy region around 3 to 4 GeV. Event rates on the narrow resonances J/ψ and ψ' are proportional to the luminosity and the energy width of the colliding beams. Typical rates are very similar for the DCI and SPEAR storage rings and are of the order of 50000 logged J/ψ events per day.

The experiments operating at these machines can be classified into two categories: magnetic (DM2,

Table 1

Properties and performance characteristics of the four major detectors measuring ψ radiative decays. A more detailed description can be found in references [10–13] and in ref. [17]. The table is divided into five parts corresponding to parameters for charged particle (c.p.) detection, neutral particle (n.p.) detection, time-of-flight (TOF) system, muon (μ) system and trigger system. Abbreviations used are: SC = spark chamber, PC = proportional chamber, DC = drift chamber, Sci = plastic scintillator, LA = liquid argon and X_0 = radiation length. σ_p references to the momentum resolution for charged tracks, σ_E is the energy resolution for electromagnetically showering particles in the electromagnetic (e.m.C) calorimeter, where p and E are in units of GeV. Typical photon efficiency values (ϵ_γ) at two energies are included. The two numbers on the solid angle coverage for e.m. particles are for the main (barrel) part and for the total detector including end-caps

	Crystal Ball	DM2	Mark II	Mark III
Magnetic field		0.50 T	0.46 T	0.40 T
Chambers	SC & PC	PC & DC	DC	2 DC's
Coil thickness		$1\ X_0$	$1.4\ X_0$	
σ_p/p		$2.5\% * \sqrt{1+p^2}$	$1.5\% * \sqrt{1+p^2}$	$1.5\% * \sqrt{1+p^2}$
$\Delta\Omega/4\pi$ (c.p.)	71–94%	87%	85%	84%
E.m. calorimeter	$16X_0$ NaI(Tl)	$6X_0$ Pb–Sci–PC	$14X_0$ Pb–LA	$12X_0$ Pb–PC
$\Delta\Omega/4\pi$ (n.p.)	93–98%	70–82%	64–78%	84–94%
σ_E/E	$2.7\%/E^{1/4}$	≈35%	$12\%/E^{1/2}$	$17\%/E^{1/2}$
σ_{θ_γ}	1–2°	0.4°	0.2–0.5°	0.6°
$\epsilon_\gamma(E_\gamma \simeq 200\,\text{MeV})$	100%	100%	50%	100%
$\epsilon_\gamma(E_\gamma \simeq 50\,\text{MeV})$	100%	50%	0	70%
σ_t(TOF)		0.31 ns	0.30 ns	0.19 ns
$\Delta\Omega/4\pi$ (TOF)		79%	75%	80%
$\pi/K(1\sigma)$		<0.7 GeV	<1.3 GeV	<1.5 GeV
$\Delta\Omega/4\pi$ (μ)		45%	50%	65%
Trigger	NaI PC	PC & DC e.m.C	Sci DC TOF	DC TOF

Mark II and Mark III) and non-magnetic (Crystal Ball) detectors. Table 1 lists the important properties and performance characteristics relevant for ψ radiative decays. Figure 1 shows as an example a typical magnetic detector, the Mark III. The magnetic detectors, being of the general-purpose type, are very well suited for analyses of final states containing a large number of charged particles in addition to few photons. They use a magnetic field of around 0.5 T produced with conventional solenoids, with the field aligned parallel to the beam. Good charged particle tracking and momentum measurement is accomplished with drift chambers over about 85 % of the total solid angle. Time-of-flight counters outside the drift chambers allow the identification of charged particles. For instance, Mark III separates π's from K's at the 1σ level up to momenta of about 1.5 GeV.

The energies of electromagnetically showering particles are measured with electromagnetic calorimeters. It is this area of particle detection where the three magnetic detectors differ considerably in their design. The lead sheet proportional counters of Mark III are placed inside the coil covering a large solid angle, whereas the other detectors register photons behind a 1 radiation length thick magnetic coil. This reduces the detection efficiency for photons with energies less than about 200 MeV. All detectors increase the solid angle coverage with end-cap shower counters. Muons are identified over about 50% of the total solid angle by proportional tubes placed behind additional absorbers. The instantaneous rate of e^+e^- interactions is determined from Bhabha scattering events measured with special luminosity counters positioned close to the beam pipe. The experiments use elaborate event triggers to determine the occurrence of e^+e^- annihilations. Trigger decisions are based on signals from the drift chamber and

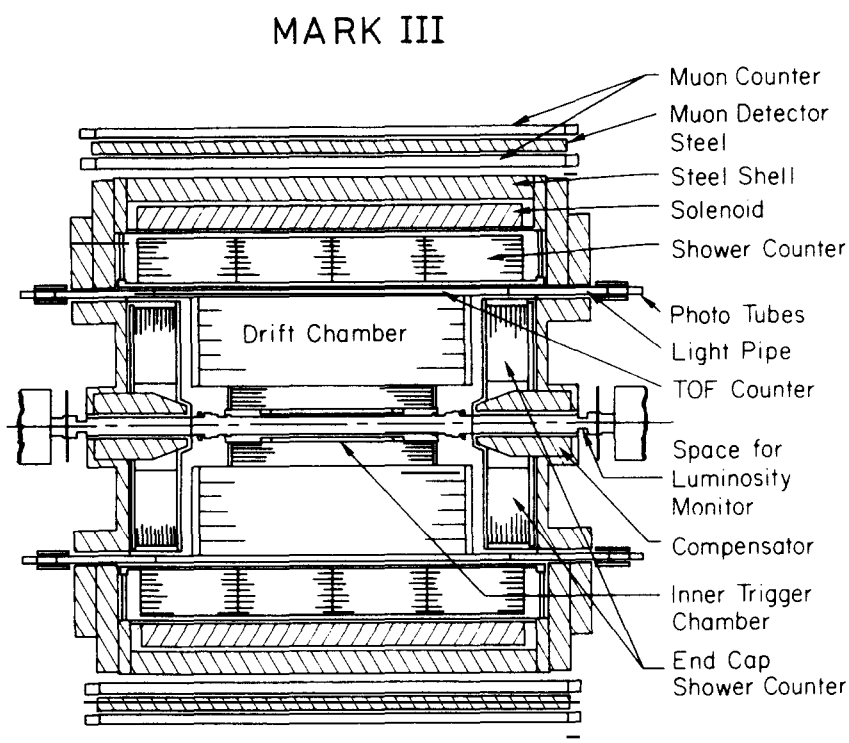

Fig. 1. Side view of the Mark III spectrometer as a typical example of a magnetic detector.

time-of-flight systems. In addition, DM2 uses information from the scintillators in the electromagnetic calorimeter for an all neutral event trigger.

The non-magnetic detector Crystal Ball (fig. 2) is optimized for high-resolution measurements of electromagnetically showering particles and is thus ideal for the study of inclusive and exclusive events containing photons. The central tracking system consisted of one proportional chamber sandwiched between two spark chambers. They covered between 71% and 94% of the full solid angle. The main part of the detector is a spherical shell made of 672 individual crystals. 93% of the solid angle is covered with the main ball; including end-caps the coverage is increased to 98%. The crystals are made of 16 radiation length thick sodium iodide doped with thallium, NaI(Tl). This thickness is sufficient to almost fully contain electromagnetic showers over the whole energy range available. The resulting energy resolution is about 4.8 MeV at 100 MeV, and the efficiency for detecting photons is 100% for energies as small as 1 MeV. Energies of muons and charged hadrons cannot be determined. A separation between hadrons, muons and electrons is possible on a statistical basis due to their different transverse energy deposition pattern in the crystals. The experiment triggers on information from the proportional chamber and the NaI shower counter. Thus charged and neutral particle triggers are available. In table 1 the parameters of this detector are compared to those from the magnetic detectors.

MARK I [18], the predecessor of the Mark II detector at the storage ring SPEAR, was the first e^+e^- experiment to observe the J/ψ. The huge, narrow production cross section clearly indicated new physics. With the announcement of this discovery on November 11, 1974, a new era began in particle physics. Only a week later this resonance was also seen at DORIS by the DASP and PLUTO collaborations. The experiment SP-27 [19] at SLAC and later DESY–Heidelberg at DORIS added valuable information.

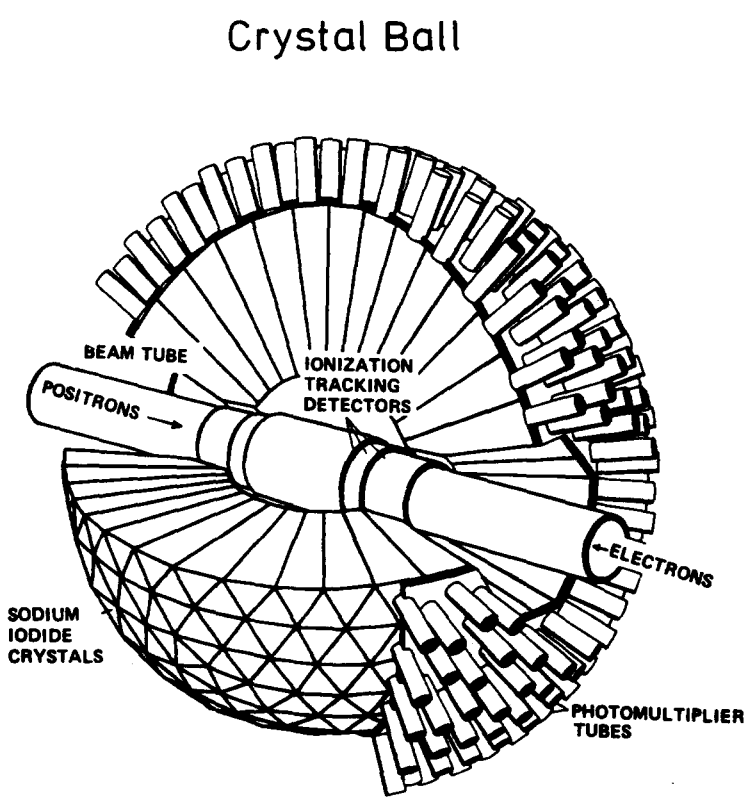

Fig. 2. Schematic of the non-magnetic Crystal Ball detector.

Table 2
Data samples taken by different detectors at the narrow resonances J/ψ and ψ'. All Mark III results are based on 2.7 million J/ψ decays with the exception of the analysis of the ξ(2200) for which the total data sample is used

Resonance	Crystal Ball	DM2	Mark II	Mark III
J/ψ	2.2×10^6	8.6×10^6	1.3×10^6	$(2.7 + 3.1) \times 10^6$
ψ'	1.8×10^6	0	1.0×10^6	0

In 1979 the Mark II detector was moved to the PEP storage ring at SLAC; in 1982 the Crystal Ball was taken to the DORIS machine at DESY. At about the same time the Mark III detector started taking data at SPEAR, followed a year later by DM2 at DCI. Table 2 summarizes the large event samples obtained by the Crystal Ball, DM2, Mark II and Mark III experiments. It is quite obvious that, more than 10 years after the J/ψ discovery, charmonium spectroscopy is still a very active field of research.

3. Radiative transitions within the charmonium system

The existence of the narrow state J/ψ was first established independently by the Mark I detector [3] at SPEAR and by a BNL–MIT group [2] at the Brookhaven National Laboratory. Even though charm was

postulated [20] in response to problems with the weak interaction, its discovery had a considerable impact on the theory of strong interactions, QCD. The pioneering papers by Appelquist and Politzer [21] and by DeRújula and Glashow [22] treated quarks for the first time as real particles bound in a QCD potential. A second resonance, the ψ′, was observed [23] shortly afterwards. As J/ψ and ψ′ are produced directly in e^+e^- interactions, they must have the quantum numbers of the photon, $J^{PC} = 1^{--}$. With the charm–anticharm quark hypothesis, two spin 1/2 quarks can form spin-singlet and spin-triplet states with total spin $S = 0$ and $S = 1$, respectively. Including angular momentum $L = 0$ and $L = 1$ yields the states shown in fig. 3. Here the spectroscopic notation is $n^{2S+1}L_J$, where n is the number of radial nodes plus one, S is the total quark spin, L is the orbital angular momentum and J is the total angular momentum of the state. Following common practice this review uses the generic names J/ψ, η_c and χ for the charmonium states $^3S_1$, $^1S_0$ and ^3P_J, respectively.

Aside from ψ′ hadronic decay modes, it was emphasized [24] to search for the radiative decay $\psi' \to \gamma\chi_c$ to three spin-triplet states with angular momentum $L = 1$. The two high mass states were discovered at DESY by the DASP experiment [25], though not resolved. Later Mark I added [26] the lowest mass χ state. Three candidates for the spin-singlet states η_c and η_c' were found [27, 28, 29]: X(2800), X(3455) and X(3590). But these states were very difficult to reconcile with the charmonium model and were subsequently ruled out by the Crystal Ball experiment. The current status of the charmonium spectrum below charm threshold is shown in fig. 3. All the observed photon transitions are indicated. Electric dipole transitions occur between states with opposite parity, whereas transitions between spin-singlet and spin-triplet states are magnetic dipole (spin-flip).

3.1. Theoretical introduction

Radiative transitions offer the possibility to produce charmonium states with quantum numbers

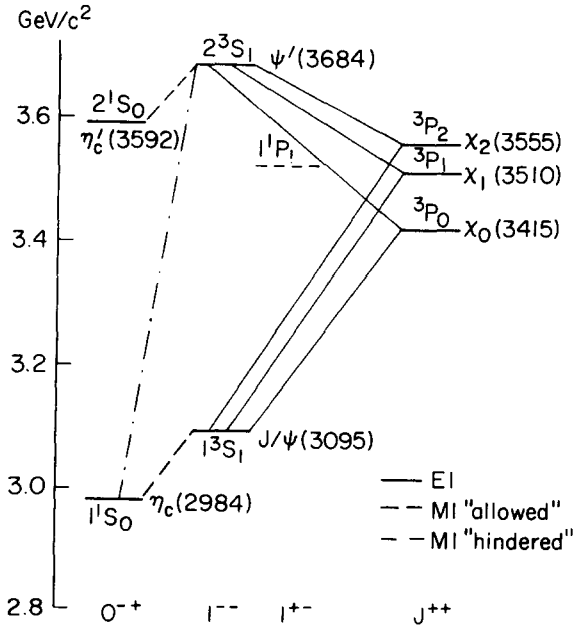

Fig. 3. The observed charmonium levels below charm threshold. The $^1P_1$ state has not yet been found. Measured radiative transitions are indicated as solid lines (electric dipole), dashed lines (magnetic dipole) and dashed–dotted lines (hindered magnetic dipole).

different from the J/ψ and ψ'. The transition matrix element is determined mostly by the wave function at large distances, where the inter-quark potential is dominated by the confining part. At the time being, QCD theory cannot provide quantitative predictions in this non-perturbative region. Therefore, investigations of radiative transitions are very important to understand the confinement of quarks. Measurements of the hadronic widths of the χ and η_c states test the picture of quark–antiquark annihilation into gluons and yield information on the wave function at the origin. The following three subsections provide some theoretical background on the potential model approach for heavy quarkonia and the predictions for radiative decay widths and hadronic widths.

3.1.1. Potential models

Quarkonia provide direct evidence for the strong binding forces between quarks. Except for Monte Carlo lattice calculations of mass spectra, QCD processes can be evaluated only as a perturbation series expansion. The first terms of this expansion should provide a good approximation as long as the expansion parameter $\alpha_s(q^2)$ is small, which happens when q^2 is large. However, many interesting aspects about hadrons involve small values of q^2, where the perturbation series does not converge. For example, to describe the mass spectra of hadrons it is appropriate to use models. These models could either be inspired by QCD or be purely phenomenological.

As the strongly interacting constituents are heavy, relativistic effects are expected to be small and a sufficiently accurate approximation may be obtained by a non-relativistic treatment. It is based on the Schrödinger equation with a static potential $V_{n.r.}$

$$\left[-\frac{1}{m_c}\nabla^2 + V_{n.r.}(r)\right]\psi(r) = E\psi(r)\,. \tag{3.1}$$

The main problem consists in choosing the correct non-relativistic potential and determining the free parameters of the potential by a fit to the data. So far the potential cannot be computed in QCD from first principles and we have to rely on models. However, numerical studies of the interquark potential have been started [30] using the lattice gauge theories of QCD. The results are in good agreement with the potentials to be discussed below.

Given the nearly equal splittings between the $2\,^3S_1$ and the $1\,^3S_1$ in charmonium and bottonium it has been suggested to use a purely phenomenological potential with a logarithmic form [31] $V(r) = C\ln(r/r_0)$ or with a powder potential [32] $V(r) = A + Br^{\epsilon}$. The two are approximately equivalent for small ϵ. The value obtained from the fits turns out to be small, $\epsilon \simeq 0.1$. Both of these potentials have been quite successful in describing the ψ states.

One of the first attempts [33] to fit the ψ mass spectrum used a potential of the form $V_{n.r.} = -\frac{4}{3}\alpha_s/r + kr$. The Coulomb-like form is suggested by lowest order QCD. It arises from one gluon exchange between quarks and dominates at short distances. The strong coupling constant α_s was either treated as a constant or was allowed [34] to depend on the momentum of the quarks. The large distance part, linear in r, is motivated by the string picture of quark confinement. In later works [35], the short-distance Coulomb and the long-distance linear potentials were connected logarithmically at intermediate distances.

Asymptotic freedom is incorporated into the potentials by softening the r-dependence [36] of the Coulomb-like term or by establishing the potential in momentum space using the QCD β-function. A particularly simple and successful example with the latter approach was suggested by Richardson [37],

$$V(q^2) = -\frac{4}{3}\,\frac{12\pi}{33-2n_f}\,\frac{1}{q^2\ln(q^2/\Lambda^2+1)}\,. \tag{3.2}$$

This potential depends only on a single scale parameter Λ as it should be the case for a true QCD potential. Note that this parameter can be related [38] directly to the scale parameter $\Lambda_{\overline{MS}}$ used in the QCD minimal subtraction scheme. Most of the models to be used below for comparison with experimental data are based on potentials defined in momentum space.

Although the procedure of constructing a potential is not unique, all approaches lead to very similar potential forms in the region of distances from about 0.1 to 1.0 fm, see fig. 4. The models begin to differ substantially for inter-quark separations less than about 0.1 fm. As long as the expected very heavy $t\bar{t}$ system is not observed, we have to search for effects which probe the very short distance region. Tests are needed which distinguish the QCD from the purely phenomenological approach. One such probe is the fine and hyper-fine splitting of charmonium.

Theoretical calculations are unfortunately not free of problems. All potential models are in some sense phenomenological as they have not been strictly derived from QCD. An exception are lattice gauge theories which, in the near future, may yield quantitative predictions for heavy quark systems [30]. Currently, QCD corrections for the potential and decays of heavy quarkonia can only be calculated in next-to-leading order. Due to the large size of the strong coupling constant α_s, these corrections are not always small enough to give a rapid convergence of the expansion series. As a result QCD predictions often have an error of 20%. Another problem concerning the correct choice of the QCD scale at which to evaluate the running coupling constant α_s. This choice [39] seems to depend more on personal intuition than on stringent physics requirements. Finally, a fully relativistic treatment has only been done for the spin 0 Klein–Gordon equation [40]. So far relativistic corrections are incorporated into the Hamiltonian up to order $(v/c)^2$. All these problems are currently being investigated.

Spin-dependent mass splittings – an intrinsically relativistic effect – are incorporated into the non-relativistic treatment by means of either the Bethe–Salpeter or the Breit–Fermi equations, where the latter is the most popular approach. The method chosen is analogous to the QED analysis of positronium. The general result given by Eichten and Feinberg [41] consists of three parts: a spin–orbit, a tensor and a spin–spin interaction term, all of them depending on the static potential. The Coulomb-like potential

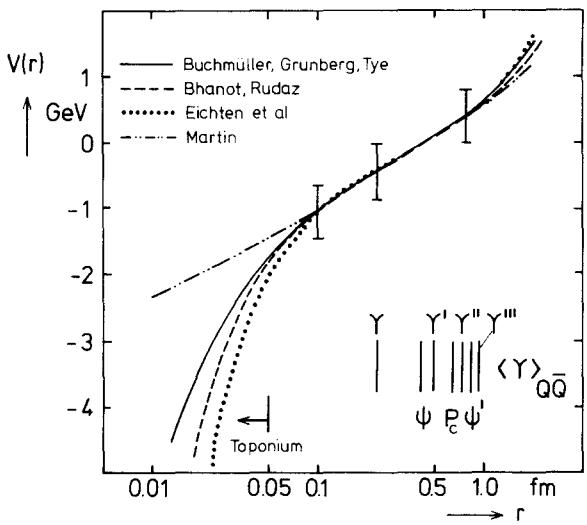

Fig. 4. The radial dependence of some typical quark–antiquark potentials for heavy quarkonia systems (from ref. [38]). The potentials have been shifted to agree at a radius of $r = 0.5$ fm. Average radii ($\sqrt{\langle r^2 \rangle}$) of the observed $c\bar{c}$ and $b\bar{b}$ states are indicated. The potential models used are by Bhanot and Rudaz (ref. [35]), Buchmüller, Grunberg and Tye (ref. [38]), Eichten et al. (ref. [33]) and Martin (ref. [32]).

arises from the exchange of a vector particle, the gluon, and therefore transforms like a Lorentz vector ($V_v \sim 1/r$). Gromes [42] has shown that the dominant contribution to the confining potential must be scalar or vector. In the analysis of Eichten and Feinberg vector confinement was assumed, yielding results different from those with scalar confinement. The latter approach by Henriques et al. [34] and Schnitzer [43] seemed to be preferred by early experimental data. This discrepancy has been resolved by Gromes [44] in favor of pure scalar confinement advocated also by Buchmüller [45] using the string picture. With a pure scalar confining potential ($V_s \sim r$) Gromes obtains

$$V_{\text{spin}}(r) = \frac{1}{2m_c^2}(\boldsymbol{L}\cdot\boldsymbol{S})\left(\frac{3V_v' - V_s'}{r}\right) - \frac{1}{3m_c^2}(3(\boldsymbol{S}_1\cdot\hat{\boldsymbol{r}})(\boldsymbol{S}_2\cdot\hat{\boldsymbol{r}}) - \boldsymbol{S}_1\cdot\boldsymbol{S}_2)\left(V_v'' - \frac{V_v'}{r}\right)$$
$$+ \frac{2}{3m_c^2}(\boldsymbol{S}_1\cdot\boldsymbol{S}_2)\nabla^2 V_v \,. \tag{3.3}$$

$\boldsymbol{L}$ is the orbital angular momentum and $\boldsymbol{S}_i$ are the quark spins. For comparison with experimental mass splittings the expectation value has to be taken of the spin-dependent potential (eq. (3.3)). With abbreviations a, b, c the general spin-dependent energies are:

$$\langle V_{\text{spin}}(r)\rangle = a\langle \boldsymbol{L}\cdot\boldsymbol{S}\rangle + b\langle 3(\boldsymbol{S}_1\cdot\hat{\boldsymbol{r}})(\boldsymbol{S}_2\cdot\hat{\boldsymbol{r}}) - \boldsymbol{S}_1\cdot\boldsymbol{S}_2\rangle + c\langle \boldsymbol{S}_1\cdot\boldsymbol{S}_2\rangle \,,$$

with

$$a = \frac{1}{2m_c^2}\left\langle\frac{3V_v' - V_s')}{r}\right\rangle; \qquad b = \frac{-1}{3m_c^2}\left\langle V_v'' - \frac{V_v'}{r}\right\rangle; \qquad c = \frac{2}{3m_c^2}\langle\nabla^2 V_v\rangle \,. \tag{3.4}$$

The ^3P_J states, which have orbital angular momentum $L = 1$ and total spin $S = 1$, are split by the spin–orbit and tensor forces only. In the case of the S states with $L = 0$ only the hyperfine term $\boldsymbol{S}_1\cdot\boldsymbol{S}_2$ contributes. An evaluation of the matrix elements of $\boldsymbol{L}\cdot\boldsymbol{S}$, $\boldsymbol{S}_1\cdot\boldsymbol{S}_2$ and the tensor term yields the mass splittings within the ^3P_J and the S states (see e.g. ref. [46]):

$$\langle V_{^3P_J}\rangle = a\begin{Bmatrix}-2\\-1\\+1\end{Bmatrix} + b\begin{Bmatrix}-1\\+\frac{1}{2}\\-\frac{1}{10}\end{Bmatrix} \quad \text{for } J = \begin{Bmatrix}0\\1\\2\end{Bmatrix},$$
$$\langle V_S\rangle = c\begin{Bmatrix}-\frac{3}{4}\\+\frac{1}{4}\end{Bmatrix} \quad \text{for } S_1 + S_2 = \begin{Bmatrix}0\\1\end{Bmatrix}. \tag{3.5}$$

With the help of these expectation values and the mass values from experiment we can derive the parameters a, b and c, and thus gain information on the potentials. For a pure Coulomb potential the hyperfine term c is a contact term ($\nabla^2 V_v$) and thus gives information on the very short-range part of the potential. b is proportional to derivatives of the vector (Coulomb) potential only. It yields direct information on the short-range behaviour of the force acting between two quarks. The a term is proportional to the expectation value of both the vector (Coulomb) and scalar (linear) potentials. It therefore yields information on the confining part of the potential.

3.1.2. Radiative widths

The easiest way to measure the fine-splitting in charmonium is to search for the radiative transitions from the ψ' to the χ states. It has been shown [47], that a dipole approximation should be adequate for the transitions. The rate is then given by [33]

$$\Gamma(\psi' \to \gamma + \chi_c) = \frac{4}{9} \frac{2J_f + 1}{2J_i + 1} q_c^2 \alpha_{em} k^3 |E_{if}|^2 , \tag{3.6}$$

where q_c is the charge of the charmed quark in units of the elementary charge e, α_{em} is Sommerfeld's fine structure constant, k is the energy of the radiated photon and $J_i(J_f)$ is the total spin of the initial (final) state. E_{if} is the transition dipole matrix element $\int R_{\psi'} r R_\chi r^2 \, dr$, with R the radial wave functions. As the ψ' wave function has a node at about 0.5 fm and the χ wave functions have none, predictions for these transitions are very sensitive to the exact position of this node. The position depends crucially on relativistic corrections which have been incorporated to order $(v/c)^2$ in the calculation by McClary and Byers [48].

Substituting the appropriate wave functions in the matrix element of eq. (3.6) yields the corresponding formula for radiative transition between χ and the ground state J/ψ. As neither wave function has a node, the predictions are rather independent of relativistic corrections and therefore more reliable.

The spin-singlet states η_c and η_c' can also be reached via radiative transition from the ψ states. The magnetic dipole rate is given by [33]

$$\Gamma(J/\psi \to \gamma + \eta_c) = \frac{16}{3} \left(\frac{q_c}{2m_c} \right)^2 \alpha_{em} k^3 |M_{if}|^2 , \tag{3.7}$$

where m_c is the charm quark mass. The rate is proportional to the Dirac magnetic moment $eq_c/2m_c$ of the quarks. The matrix element M_{if} is defined by $M_{if} = \int R_\psi R_{\eta_c} j_0(kr/2) r^2 \, dr$, where j_0 is the spherical bessel function of order zero. In the non-relativistic limit, the wave functions of J/ψ and η_c are identical. With $j_0(kr/2 \ll 1) \simeq 1$, the matrix element is expected to be close to one and relativistic corrections [49] turn out to be small. On the other hand, the 'hindered' transition $\psi' \to \gamma + \eta_c$ involves orthogonal wave functions. Rate calculations depend strongly on relativistic effects and coupled channel mixing.

3.1.3. Hadronic widths

The main energetically allowed hadronic decays of the ψ states require the c and $\bar{c}$ quarks to annihilate into light hadrons. According to the recipe by Appelquist and Politzer [50, 22] this process proceeds in lowest-order QCD through a two- or three-gluon intermediate state which fragment into hadrons. The annihilation rates depend strongly on the angular momentum and spin of the charmonium states under consideration. The minimal number of gluons for the decay of a C-odd state like the J/ψ is three gluons. For C-even parity states like the η_c and χ the decay is via two and three gluons. In lowest order the two-gluon decay should be dominant where allowed.

Lowest-order QCD calculations yield the following formulas for the decay widths [50, 51]:

$$\Gamma(J/\psi \to ggg) = \frac{40}{81\pi} (\pi^2 - 9) \alpha_s^3 \frac{|R_{J/\psi}(0)|^2}{M_{J/\psi}^2} , \tag{3.8}$$

$$\Gamma(\eta_c \to gg) = \tfrac{8}{3} \alpha_s^2 |R_{\eta_c}(0)|^2 / M_{\eta_c}^2 , \tag{3.9}$$

$$\Gamma(\chi_0 \to gg) = 96\alpha_s^2 \, |R'_{\chi_0}(0)|^2 / M^4_{\chi_0} , \tag{3.10}$$

$$\Gamma(\chi_1 \to q\bar{q}g) = \frac{n_f}{3} \frac{128}{3\pi} \alpha_s^3 \frac{|R'_{\chi_1}(0)|^2}{M^4_{\chi_1}} \ln\left(\frac{4m_c^2}{4m_c^2 - M^2_{\chi_1}}\right), \tag{3.11}$$

$$\Gamma(\chi_2 \to gg) = \frac{128}{5} \alpha_s^2 \frac{|R'_{\chi_2}(0)|^2}{M^4_{\chi_2}} , \tag{3.12}$$

where n_f is the number of light quark flavors ($n_f = 3$ for charmonium) and $R(0)$ is the radial part of the wave function at the origin (or its derivative for the χ decays). Note that sometimes these widths are written in terms of the *total* wave function at the origin. This introduces a factor of 4π into the above formulae. The decay width for the χ_1 state is different from the other χ states because a spin 1 particle is forbidden to decay to two massless vector particles [52]. The $q\bar{q}g$ channel dominates over the also allowed ggg channel and yields the above stated width [51]. The logarithm in the decay $\chi_1 \to q\bar{q}g$ is due to a threshold singularity in the limit of zero binding energy.

Next-to-leading order calculations [53] have been performed for the χ_0 and $\chi_2$widths. It is useful to consider their ratio, where the *a priori* unknown derivative of the wave function divides out. The result is [53]

$$\Gamma(\chi_0 \to gg)/\Gamma(\chi_2 \to gg) = \tfrac{15}{4}(1 + 12\alpha_s/\pi) . \tag{3.13}$$

Typical lowest-order predictions for the widths vary between 50 keV for the J/ψ and 5 MeV for the η_c.

3.2. The charmonium χ states

This section covers results for the E1 transitions $\psi' \to \gamma\chi$ and $\chi \to \gamma J/\psi$. Most of the experimental results have been described in detail in the review article by Bloom and Peck [10]. A summary is given here with particular stress on new experimental data and new theoretical information. This section is divided into two parts. The first part summarizes experimental results on branching ratios, masses and widths of the χ states. The second part compares the obtained parameters with theoretical predictions. Conclusions are drawn regarding QCD predictions and relativistic corrections.

3.2.1. Experimental results

The χ_c states are produced in radiative decays of the ψ'. There are three approaches to study these transitions. The first method consists in searching for decays of the ψ' into one photon plus hadrons, e.g., $\psi' \to \gamma\pi^+\pi^-\pi^+\pi^-$. It is mostly employed by magnetic detectors and yields precise χ mass values by reconstructing the invariant mass of the hadronic system. In addition, this method allows for a determination of the total width of the χ states.

To determine radiative branching ratios a second method has to be employed. It consists of measuring the inclusive photon energy distribution in hadronic decays of the ψ'. Initially, magnetic detectors have analyzed converted photons [54], but the efficiency for this technique is rather small. The measurement of radiative branching ratios is done best with electromagnetic calorimeters, identifying photons and their energies with large efficiency and high precision, respectively. The first such detector was SP-27 [19] at SPEAR. Using 19 NaI crystals arranged around the interaction region they succeeded in measuring the

inclusive radiative branching ratios. In the fall of 1978, a dedicated neutral particle detector covering a large solid angle, the Crystal Ball, started operating. Its excellent photon measurement capabilities yielded precise branching ratios [55]. Figure 5 shows the inclusive photon spectrum obtained by the Crystal Ball experiment. Prominent peaks (labeled 2, 3 and 4) correspond to the transitions to the χ states. The inclusive radiative branching ratios obtained by all experiments are summarized in table 3.

The third method to determine the χ states consists of measuring the cascade process $\psi' \to \gamma\chi$, $\chi \to \gamma J/\psi$. Here the J/ψ is identified by its decay to $\mu^+\mu^-$ or e^+e^-. The magnetic detector experiments Mark I, Mark II, and DASP as well as the non-magnetic detectors DESY–Heidelberg and Crystal Ball identified this process. Results are included in table 3. Both detector types yield very similar values for the product branching ratios. The branching ratios BR($\chi \to \gamma J/\psi$) have been calculated from the average values of the inclusive and exclusive measurements, and the results are shown in the last row of table 3. In addition, the data from the Crystal Ball experiment yielded high confidence levels for the spins [58] of $\chi_{1,2}$ as preferred in the charmonium model, i.e., $J = 1$ and 2 for χ_1 and χ_2, respectively. Note that the spin

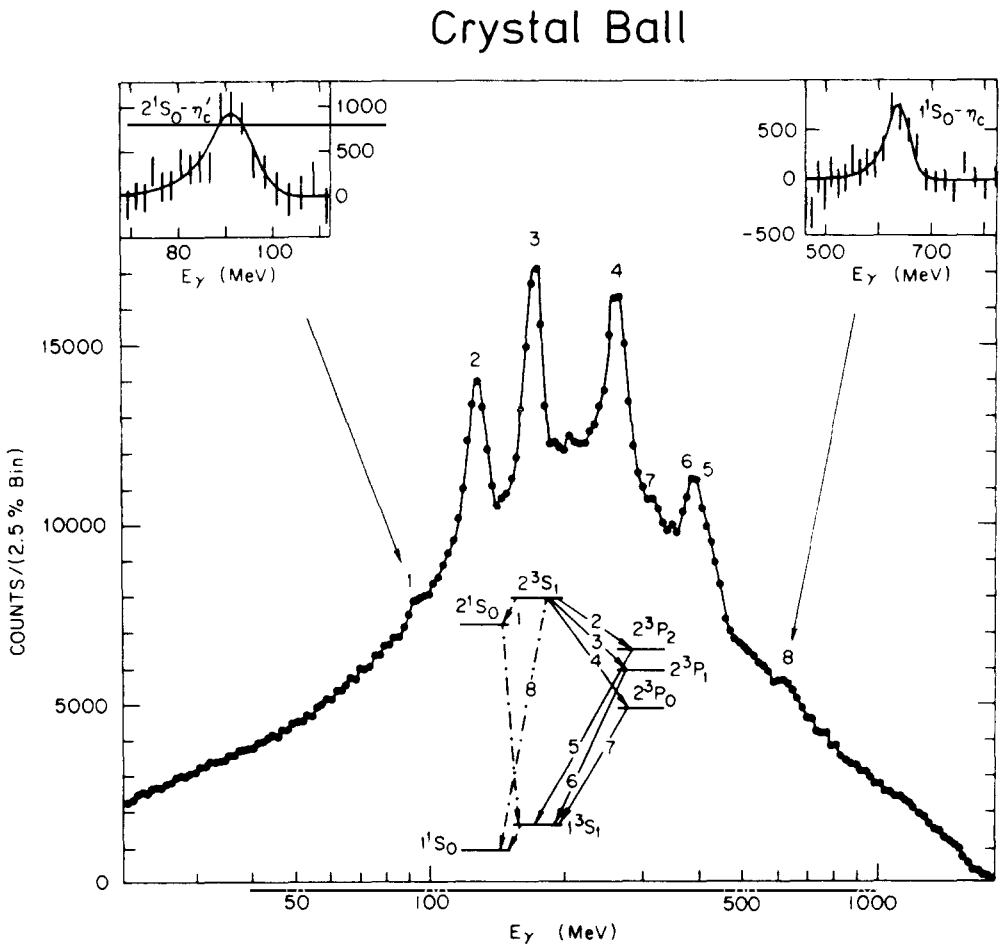

Fig. 5. Inclusive photon spectrum at the ψ′ obtained by the Crystal Ball experiment. Note that the logarithmic energy scale yields bin sizes approximately proportional to photon energy resolution. The numbers over the spectrum correspond to the expected radiative transitions shown in the spectrum inset.

Table 3
Branching ratios for the radiative decays of the ψ′ to the χ states and the product branching ratios for the decays further down to the J/ψ. Systematic and statistical errors have been added in quadrature. Weighted averages have been formed. The branching ratios BR(χ→γJ/ψ) have been calculated, where errors from the branching ratios BR(ψ′→γχ) have not be been included. This introduces an additional 10% scale error

BR(ψ′→γχ) (%)				
Experiment	χ_0	χ_1	χ_2	Ref.
Mark I	7.5 ± 2.6			[54]
SP-27	7.2 ± 2.3	7.1 ± 1.9	7.0 ± 2.0	[19]
Crystal Ball	9.9 ± 0.9	9.0 ± 0.9	8.0 ± 0.9	[55]
Average	9.4 ± 0.8	8.6 ± 0.8	7.0 ± 0.8	
BR(ψ′→γχ, χ→γJ/ψ) (%)				
Experiment	χ_0	χ_1	χ_2	Ref.
Mark I	0.2 ± 0.2	2.4 ± 0.8	1.0 ± 0.6	[54]
DESY-HD	0.14 ± 0.09	2.5 ± 0.4	1.0 ± 0.2	[56]
DASP	0.3 ± 0.2	1.7 ± 0.4	1.4 ± 0.4	[14]
Mark II	<0.56	2.4 ± 0.6	1.1 ± 0.3	[57]
Crystal Ball	0.06 ± 0.02	2.4 ± 0.4	1.3 ± 0.2	[58]
Average	0.07 ± 0.02	2.2 ± 0.2	1.2 ± 0.1	
BR(χ→γJ/ψ) (%)				
Average	0.74 ± 0.21	25.6 ± 2.3	15.4 ± 1.3	

assignments are also supported [59] by the hadronic decay modes of the χ states. Finally, the transitions between the ψ′ and $\chi_{1,2}$ were shown by the Crystal Ball [58] to be predominantly electric dipole.

Table 4 collects mass and width determinations for the χ states. Mass values determined from analyses of hadronic χ decays are included from the Particle Data Group [59]. A new measurement of the total width of the χ_0 has been obtained by the Crystal Ball group [60] analyzing the decay $\chi_0 \to \pi^0\pi^0$. The last ISR experiment R704 [61] used the technique of $p\bar{p}$ annihilation and scanning the beam energy over the expected mass region of the χ states. With a mass resolution of 0.3 MeV they succeeded in measuring χ_1 and χ_2 mass values and the χ_2 width, as shown in table 4.

Table 4
Masses and widths of the χ states in MeV. Systematic and statistical errors have been added in quadrature. Measurements of the χ masses in hadronic decays are taken from the Particle Data Group summary (which also includes the mass determinations by the Crystal Ball [58]). Upper limits and confidence intervals are at the 90% confidence level, except for R704 results where the levels are 95%. The average for $\Gamma(\chi_0)$ has been calculated in ref. [55]

	Mass (MeV)			Γ(χ) (MeV)			
	χ_0	χ_1	χ_2	χ_0	χ_1	χ_2	Ref.
Hadronic average	3415.0 ± 1.0	3510.0 ± 0.6	3555.8 ± 0.6				[59]
R704		3511.4 ± 0.5	3556.8 ± 0.6		<1.3	3^{+2}_{-1}	[61]
Crystal Ball	3417.9 ± 4.3	3512.3 ± 4.2	3557.8 ± 4.1	13–21	<4	1–5	[55]
Crystal Ball	3415.6 ± 1.4	3510.4 ± 0.6	3555.9 ± 0.7	9 ± 2	<2.6	4 ± 1	[58, 60]
Average	3415.3 ± 0.8	3510.8 ± 0.4	3556.3 ± 0.4	13 ± 5	<1.3	3.6 ± 0.7	

3.2.2. Comparison with theory

According to the results presented above, the comparison with theory is divided into three parts: comparison with radiative branching ratios, hadronic widths and χ masses. In table 5 selected predictions on $\psi' \to \gamma\chi$ and $\chi \to \gamma J/\psi$ widths are compared with experimental data. As the spin-dependent long-range potential has been shown to transform like a scalar under Lorentz transformations (see section 3.1.1), only theories incorporating scalar confinement are used for comparison. Predictions have been adjusted for the measured photon energies. The experimental widths are calculated using the total width of the ψ′ of (215 ± 40) keV [59] and the χ (see table 4). A 19% scale error from the uncertainty in the total width of the ψ′ has not been included.

The agreement between theory and experiment is satisfactory. Early non-relativistic predictions on $\Gamma(\psi' \to \gamma\chi)$ were too large by a factor of two. This discrepancy was solved by McClary and Byers [48]. Inclusion of relativistic $(v/c)^2$ corrections and coupled channel (c.c.) effects reduce the predicted width to a value compatible with experiment, see table 5 for the development by successive inclusion of these effects. The influence of relativistic corrections on the transition rate $\chi \to \gamma J/\psi$ rate is much smaller as both wave functions have no nodes. Note also the good agreement with one of the earliest theories incorporating scalar confinement, the prediction by Henriques et al. [34]. As an example of the sum-rule approach of QCD, the prediction by Novikov et al. [47] is included. The agreement with data is very good. A bag model calculational by Baacke et al. [62] yields comparable values.

Table 6 shows the average hadronic width together with theoretical predictions. Note that the comparison is done for hadronic and not total widths; they are related by $\Gamma_{\text{had}} = \Gamma_{\text{tot}}(1 - \text{BR}(\chi \to \gamma J/\psi))$. Barbieri et al. [51] derived and Olsson et al. [65] used the formulae for hadronic widths given in eqs. (3.10)–(3.12) with an estimate of the derivative of the χ wave function at the origin obtained from potential models. The predictions seem too low for the χ_0 and χ_2 widths. But these width calculations are subject to large QCD radiative corrections [53]. In lowest-order QCD the ratio of the χ_0 to χ_2 width is given by $\frac{15}{4} = 3.75$ (eq. (3.13)), very close to the experimental ratio of 4.2 ± 1.8. First-order QCD yields a value of 6.9, but inclusion of (unknown) higher orders might bring this ratio down again. The QCD sum-rule calculations by Novikov et al. [47] yield hadronic widths about a factor of two higher than those from potential models, but still do not meet the χ_0 experimental width. The deviation between theory and experiment on the χ hadronic width is one of the remaining problems in the $c\bar{c}$ system. It has been speculated [65], but not yet proven, that this is due to relativistic effects distorting the wave functions.

Table 5

Comparison of the experimental radiative widths with theoretical predictions. The experimental values are determined from the average branching ratios (table 3) and the total widths of the ψ′ (215 keV) and χ (table 4). The predictions by McClary and Byers [48] are shown for the non-relativistic approximation (n.r.) and including $(v/c)^2$ and coupled channel (c.c.) corrections

	$\Gamma(\psi' \to \gamma\chi)$ (keV)			$\Gamma(\chi \to \gamma J/\psi)$ (keV)			Ref.
	χ_0	χ_1	χ_2	χ_0	χ_1	χ_2	
Experiment	20.2 ± 1.7	18.5 ± 1.7	16.8 ± 1.7	96 ± 46	<405	555 ± 130	
Baacke et al.	24	27	25	162	328	415	[62]
McClary et al. (n.r.)	45	40	27	121	250	362	[48]
McClary et al. $(v/c)^2$	19	31	27	128	270	347	[48]
McClary et al. (c.c.)	16	23	22	117	240	305	[48]
Falkensteiner et al.	22	32	24	111	225	306	[63]
Grotch et al.	17	27	27	167	352	427	[64]
Henriques et al.	22	21	14	120	258	367	[34]
Novikov et al.	25	19	14	210	463	603	[47]

Table 6
Hadronic widths of the χ states

$\Gamma_{had}(\chi)$ (MeV)	χ_0	χ_1	χ_2	Ref.
Experiment	13 ± 5	<1.0	3.1 ± 0.6	
Novikov et al.	4–5	0.7–3.5	1.6–2.2	[47]
Barbieri et al.	2.4		0.64	[51]
Olsson et al.	~2.5	~0.2	~0.7	[65]

Another test of QCD is the measurement of the two-photon decays of the χ_0 and χ_2. The branching fractions have been determined by the Crystal Ball group [60] to

$$\mathrm{BR}(\chi_0 \to 2\gamma) = (3.9 \pm 2.2) \times 10^{-4}\,, \qquad \mathrm{BR}(\chi_2 \to 2\gamma) = (9.0 \pm 3.8) \times 10^{-4}\,.$$

To eliminate the dependence on the uncertain χ total widths it is best to compare ratios of branching fractions. The experimental result for $\mathrm{BR}(\chi_2)/\mathrm{BR}(\chi_0)$ is 2.3 ± 1.6. The theoretical prediction [51], corrected for the observed branching fraction of $\chi_c \to \gamma J/\psi$, is 0.85 in lowest order QCD. Including first-order corrections [53] raises it to 1.2, quite compatible within the large experimental uncertainty.

The remainder of this section is devoted to an evaluation of theoretical predictions on the χ masses. As discussed in section 3.1.1. the averaged spin-dependent part of the potential can be written (eq. (3.4))

$$\Delta M_{\mathrm{spin}} \equiv \langle V_{\mathrm{spin}}(r) \rangle = a\langle \boldsymbol{L} \cdot \boldsymbol{S} \rangle + b\langle T_{12} \rangle + c\langle \boldsymbol{S}_1 \cdot \boldsymbol{S}_2 \rangle\,,$$

where the last term, the hyperfine part, is constant for the χ states under consideration. It is customary to define a ratio $r = (M_2 - M_1)/(M_1 - M_0)$ where M_J are the masses for the states with total spin J. In terms of a and b this ratio is given by $r = (2a - 0.6b)/(a + 1.5b)$. Given the accuracy of today's world average values for the χ masses it is more appropriate to study the individual parameters a and b instead of the ratio r. With the averaged χ masses from table 4 the following values for the parameters a and b are obtained:

$$a = \frac{1}{2m_c^2}\left\langle \frac{3V_v' - V_s'}{r} \right\rangle = (34.9 \pm 0.2)\ \mathrm{MeV}\,, \qquad b = \frac{-1}{3m_c^2}\left\langle V_v'' - \frac{V_v'}{r} \right\rangle = (40.4 \pm 0.6)\ \mathrm{MeV}\,.$$

Setting the long-range potential to zero would retain the spin dependence as in pure QED. With the standard Coulomb force this yields the relation $a = 1.5b$ (QED). The experimental values in table 7 indicate that the heavy $b\bar{b}$ system with $a \simeq 1.3b$ is closer to this value than the $c\bar{c}$ system. In charmonium, the relation $a \simeq 0.9b$ reveals the importance of the long-range component of the force.

For comparison with theory the corresponding parameters are collected in table 7. Also given are the values determined for the lowest $b\bar{b}$ χ_b states [66]. The model by Gupta et al. [67], which includes higher-order QCD corrections, is in excellent agreement with the data. The QCD sum-rule approach [68], which is so successful in predicting the J/ψ–η_c hyperfine splitting, does not reproduce well the fine-structure splitting in the χ system. Predictions on the χ center-of-gravity (COG) are for some models off by up to 30 MeV. But this is due to an over- or underestimate of the long-range force component and not of the spin splittings. Together with the experimental splittings in the $b\bar{b}$ system, the relative strength of the short- and long-range force has become better understood.

Table 7
Expectation values of the spin-orbit (a) and tensor (b) potential terms as determined from the experimental and theoretical χ masses. Included are the corresponding values for the bottonium system for comparison

Origin	a (MeV)	b (MeV)	r	Ref.
χ ($c\bar{c}$) (expt.)	34.9 ± 0.2	40.4 ± 0.6	0.48 ± 0.01	
Baacke et al.,	30.7	25.6	0.67	[62]
Buchmüller et al.	35.1	31.9	0.61	[38]
McClary et al.	33.1	48.6	0.35	[48]
Falkensteiner et al.	39.1	35.3	0.62	[63]
Grotch et al.	28.2	23.9	0.66	[64]
Gupta et al.	35.7	42.2	0.46	[67]
Henriques et al.	30.0	33.3	0.50	[34]
Reinders et al.	41.7	38.9	0.60	[68]
χ($b\bar{b}$) (expt.)	14.3 ± 0.5	11.3 ± 1.1	0.70 ± 0.07	[66]

Together with the bottonium χ_b states it can be shown [69], that purely phenomenological models [32] fail to reproduce COG and splittings. This fact can be viewed as a success for the potentials based on QCD. They seem to have the right ingredients like one-gluon exchange, asymptotic freedom and linear confinement. Therefore these models should in principle allow a determination of the only scale-parameter in QCD, $\Lambda_{\overline{MS}}$. Indeed Buchmüller et al. [38] have found a lower bound on the scale parameter of QCD, $\Lambda_{\overline{MS}} > 100$ MeV, from an analysis of the charmonium and bottonium data. Recently, Hagiwara et al. have re-analyzed [70] these data including the χ_b' states. They obtain $\Lambda_{\overline{MS}} = 250 \pm 100$ MeV, a value equal to that obtained by an analysis [39] of all processes which measure the running coupling constant of QCD. Summarizing, all measurements with the exception of the total width of the χ_0 are reproduced rather well in the different models.

3.3. The charmonium η_c and η_c' states

In this section results are presented for the magnetic dipole transitions from the spin-triplet to the spin-singlet states. Experimental results on the branching ratios $BR(J/\psi \to \gamma\eta_c)$, $BR(\psi' \to \gamma\eta_c)$, $BR(\psi' \to \gamma\eta_c')$ and the masses and widths of η_c and η_c' are presented in part one. These results are then compared with theoretical predictions in the second part.

3.3.1. Experimental results

The lowest-lying $c\bar{c}$ bound state, the pseudoscalar state η_c, has been the object of considerable search ever since the discovery of the vector state J/ψ. Early observations [27] of a 2γ peak at a mass of 2830 MeV in the decay mode $J/\psi \to 3\gamma$ were not confirmed [71] in a subsequent experiment by the Crystal Ball collaboration. Later, this group found evidence [55, 72] for a new candidate state at (2984 ± 5) MeV in the inclusive photon spectra of both the J/ψ and ψ'. The inset in fig. 5 shows the observed signal in the spectrum from the ψ'. The radiative branching ratios and the η_c width were determined [55]:

$$BR(J/\psi \to \gamma\eta_c) = (1.27 \pm 0.36)\% , \qquad BR(\psi' \to \gamma\eta_c) = (0.28 \pm 0.06)\% ,$$
$$\Gamma_{tot}(\eta_c) = (11.5 \pm 4.5)\,\text{MeV} . \tag{3.14}$$

In addition this experiment obtained evidence for the decay of the η_c into $\eta\pi\pi$. Confirming evidence on the η_c came from the Mark II collaboration [73]. They observed four hadronic decay modes in $\psi' \to \gamma\eta_c$: $\eta_c \to K_s^0 K^{\pm}\pi^{\mp}$, $\pi^+\pi^-\pi^+\pi^-$, $\pi^+\pi^- K^+ K^-$, $p\bar{p}$.

A candidate for the radial excitation of the η_c, the η_c', was discovered by the Crystal Ball experiment [74] at a mass of (3594 ± 5) MeV with an inclusive radiative branching ratio and a width of

$$BR(\psi' \to \gamma\eta_c') = (0.2\text{–}1.3)\%\ (95\%\ \text{CL}), \qquad \Gamma_{tot}(\eta_c') < 8\ \text{MeV}. \tag{3.15}$$

It was not until the Mark III and DM2 groups accumulated large data sets at the J/ψ that more information on the η_c became available. A Mark III analysis of the $\eta_c \to \phi\phi$ decay angular distributions provided the first experimental determination [75] of the spin-parity of the η_c. The result, $J^P(\eta_c) = 0^-$, agrees with expectation. The DM2 $\phi\phi$ data were also shown to be consistent [76] with a 0^- hypothesis.

From a detailed study of 2.7 million J/ψ decays, the Mark III collaboration determined more accurate branching ratios [77] for the previously measured decays (see above) and found three new modes: $\eta_c \to \eta'\pi^+\pi^-$, $K^{*0}K^{\pm}\pi^{\mp}$ and $K^{*0}\bar{K}^{*0}$. Upper limits on selected decay channels were also obtained. Table 8 states the average of all experimental branching ratios divided by the inclusive $BR(J/\psi \to \gamma\eta_c)$ given above. Isospin factors have been taken into account assuming the η_c to be an iso-singlet. This assumption is justified by the observed strengths of the different $K\bar{K}\pi$ modes [77].

3.3.2. *Comparison with theory*

Summing all branching ratios in table 8 shows that approximately 21% of all η_c decay modes have been observed so far. The experimental branching ratios are in rough agreement with a prediction by Quigg and Rosner [78] using a statistical model with a Poisson multiplicity distribution. Haber and Perrier [79] tried to relate different decays of the η_c to two vector mesons. The analysis is complicated by the presence of three η_c decay mechanisms, where the η_c annihilates into two gluons which couple in different ways to the two vector mesons. Given the experimental results, it seems that the rate increases with the number of

Table 8

Mass of the η_c and branching ratios to hadronic final states. All measurements were obtained in radiative J/ψ decays except those by the Mark II collaboration. The inclusive radiative branching fractions measured by the Crystal Ball were taken to obtain the η_c hadronic branching ratios, which results in an additional 28% scale error. Weighted averages were formed if more than one experimental results exists

Decay mode X	$BR(\eta_c \to X)(\%)$	Refs.
$\eta\pi\pi$	5.1 ± 1.1	[72, 77]
$\eta'\pi\pi$	4.2 ± 1.3	[77]
$K\bar{K}\pi$	5.5 ± 0.9	[73, 77, 76]
$2(\pi^+\pi^-)$	1.3 ± 0.5	[73, 77]
$\pi^+\pi^- K^+K^-$	2.0 ± 0.3	[73, 77]
$K^{*0}K^-\pi^+ + \text{c.c.}$	2.0 ± 0.5	[77]
$K^*\bar{K}^*$	0.9 ± 0.5	[77]
$\phi\phi$	0.4 ± 0.1	[75, 76]
$p\bar{p}$	0.13 ± 0.06	[73, 77]
$M(\eta_c)$ (MeV)	2979.4 ± 1.3	[72, 73, 77]

strange quarks in the final state – quite in contrast to what is known of J/ψ decays. A detailed understanding of the dynamics of η_c decays is still missing.

In table 9 three theoretical calculations are compared with the experimental widths. The latter are obtained by multiplying the corresponding radiative branching ratios by the total widths [59] of J/ψ and ψ′. The theoretical predictions are based on potential models [49, 64] and the sum-rule approach [80] in QCD. An estimate using the non-relativistic radiative M1 width formula (eq. (3.7)) with a charmed quark mass of $m_c = 1.8$ GeV yields $\Gamma(J/\psi \to \gamma\eta_c) = 2.0$ keV and $\Gamma(\psi' \to \gamma\eta_c') = 1.0$ keV. Whereas the last value is well within the experimentally allowed range, the former value is about a factor of two too large.

In fact, most theoretical predictions yield values for the width $J/\psi \to \gamma\eta_c$ in the range of 1 to 2 keV, a little too large with respect to the experimental datum. As the theoretical width is proportional to the Dirac magnetic moment, smaller widths can be obtained at the expense of large charmed quark masses. But masses much larger than 1.8 GeV are not allowed by potential model calculations. Grotch et al. [64] have tried the assumption of a large anomalous magnetic moment for charmed quarks. Smaller widths can be obtained, see the predictions in parentheses in table 9. However, such a large anomalous quark moment does not seem to be reasonable.

The situation is much better for the transition width $\psi' \to \gamma\eta_c'$. All predictions yield values which are compatible within the large range allowed by the experimental limit. For the radiative width $\psi' \to \gamma\eta_c$ the calculational difficulties are quite different. It has been mentioned in section 3.1.2 that this is a hindered M1 transition, as the wave functions of ψ′ and η_c are orthogonal. Only relativistic corrections will allow for a finite width. In potential models the width can be made to agree with experiment by inclusion of relativistic corrections and coupled channel effects. In the calculation of Zambetakis and Byres et al. [49] this reduces the width from 3.7 to 0.3 keV. In contrast, the standard sum-rule approach predicts too small a value of 0.04 keV. A remedy suggested by Shifman and Vysotsky [80] is to assume that the decay proceeds through a gluon admixture in the ψ′ wave function and in addition to require a large $\psi'' \to \gamma\eta_c$ amplitude. Unfortunately the latter hypothesis cannot easily be tested.

The width of the η_c has been predicted between 4.2 MeV and 7.3 MeV, to be compared with the experimental datum of (11.5 ± 4.5) MeV. The lower theoretical value has been obtained by Shifman et al. [80] with an estimated uncertainty of 1 MeV. By relating the hadronic width of the J/ψ and η_c (eqs. (3.8) and (3.9):

$$\Gamma(\eta_c \to 2g) = \frac{27\pi}{5(\pi^2 - 9)} \frac{1}{\alpha_s} \Gamma(J/\psi \to 3g) \simeq 100\Gamma(J/\psi \to 3g),$$

a value of about 4.1 MeV is obtained with $\alpha_s = 0.2$. Incorporating first-order QCD radiative corrections,

Table 9
Comparison of the experimental radiative widths with theoretical pedictions. The experimental values are determined from the branching ratios given in eqs. (3.14) and (3.15) using total widths [59] for the J/ψ and ψ′ of 63 keV and 215 keV, respectively. This introduces an additional scale uncertainty of 14% and 19%, respectively

Γ (keV)	$J/\psi \to \gamma\eta_c$	$\psi' \to \gamma\eta_c$	$\psi' \to \gamma\eta_c'$	Ref.
Experimental	0.80 ± 0.23	0.60 ± 0.17	0.43–2.8	
Zambetakis et al.	2.2	3.7–0.3	0.75	[49]
Grotch et al.	1.2 (0.4)	8.4 (0.4)	0.2 (0.6)	[64]
Shifman et al.	2.2–3.2	0.75	~1.6	[80]
Non-relativistic M1	2.0	~0	1.0	[33]

Barbieri et al. [53] obtain $\Gamma(\eta_c) \simeq 7.3$ MeV. This latter value is in agreement with the experimental width, although one may wonder about the magnitude of the second-order QCD correction.

The measurement of the 2 photon decay width of the η_c is another test of QCD. The Crystal Ball [81] upper limit of $\Gamma(\eta_c \to 2\gamma) < 15$ keV is well above theoretical predictions ranging from 4 keV (sum-rules [68]) to 7.5 keV (potential model with QCD corrections [53]). The R704 experiment has presented [61] preliminary evidence for the observation of this decay; the deduced width is about ~4 keV, consistent with theory. Recently, PLUTO [82] has determined the two-photon width of the η_c in photon–photon scattering processes. They obtain $\Gamma(\eta_c \to 2\gamma) \times \mathrm{BR}(\eta_c \to K_s K^{\pm}\pi^{\mp}) = (0.5 \pm 0.2)$ keV, where statistical and systematic error have been averaged. Dividing out the hadronic branching ratio (table 8) yields $\Gamma(\eta_c \to 2\gamma) = (27 \pm 13)$ keV, compatible with theory given the large experimental errors.

Using QCD sum-rules, the mass of the η_c had been predicted [80] by the ITEP group to be 2977 MeV. It was argued [80] at the time of the wrong η_c that "the recipe of Applequist and Politzer and the whole non-relativistic approach to radiative decays in charmonium must be wrong", if the X(2800) were to survive. Fortunately, the real η_c was found at a mass of 2980 MeV, incredibly close to the prediction. Potential models like to put this spin-singlet state in the mass range from 2975 MeV to 3000 MeV. Including first-order radiative corrections [53] lead to a mass value of about 3040 MeV, but again, the corrections are rather large (45%) and higher orders might change the first-order correction substantially. Summarizing it seems that, except for a slight problem with the radiative width $J/\psi \to \gamma\eta_c$, all experimental measurements are well reproduced within such different approaches as potential models and sum-rules.

4. Radiative decays to pseudoscalar particles

The main energetically allowed decay modes of the J/ψ require the c and $\bar{c}$ quarks to annihilate, shown in figure 6. The decay mode with the largest rate is described in lowest order QCD by a three gluon intermediate state (fig. 6a). The partial width is calculated to (see section 3.1.3)

$$\Gamma(J/\psi \to ggg) = \frac{40}{81\pi}(\pi^2 - 9)\alpha_s^3 \frac{|R_{J/\psi}(0)|^2}{M_{J/\psi}^2}, \tag{4.1}$$

where $\alpha_s(q^2)$ is the strong coupling constant to be evaluated at the scale $q = 0.44 M_{J/\psi}$ [83], $M_{J/\psi}$ is the

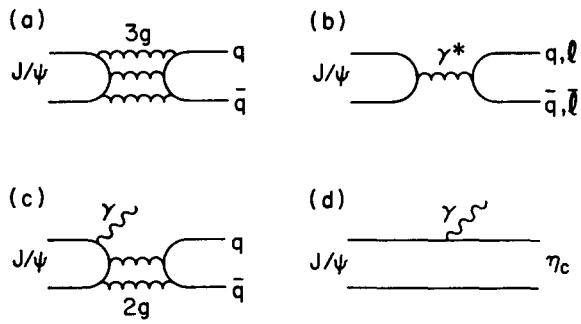

Fig. 6. Feynman diagrams for J/ψ decay: (a) three-gluon decay; (b) electromagnetic decay to leptons and quarks; (c) radiative decay to two gluons and (d) radiative decay to η_c.

mass of the J/ψ resonance, and $R_{J/\psi}(0)$ is the J/ψ radial wave function at the origin. The three-gluon decay branching ratio has been determined [33] in potential models to about 60%. Obviously, other decay channels are competing strongly with this mode.

The second largest rate turns out to be the decay to a virtual photon, which couples to quarks and leptons (fig. 6b). Given a J/ψ mass of 3.097 GeV, the only allowed leptonic final states are electron and muon pairs. In the limit $m_{e,\mu} \ll M_{J/\psi}$ both rates will be identical. The measured branching ratio to leptons is [59] $BR_{\mu\mu} \simeq 7.4\%$. The virtual photon decay rate to quarks which fragment into hadrons is R times the leptonic rate, where R measures the normalized hadronic cross section in e^+e^- annihilations off the J/ψ resonance:

$$R = \frac{\sigma(e^+e^- \to \text{hadrons})}{\sigma(e^+e^- \to \mu^+\mu^-)} .$$

Using [59] $R \simeq 2.2$ yields $BR_{\gamma^* \to had} \simeq 16\%$.

The magnetic dipole radiative decay mode $J/\psi \to \gamma\eta_c$ (fig. 6d) has been treated in detail in section 3.3. Its branching ratio has been measured to 1.3%. Summing the theoretical (ggg) and the experimental ($\mu\mu$, $\gamma^* \to$ had and $\gamma\eta_c$) branching ratios gives about 90%. The missing decay channel contributing another 10% is depicted in fig. 6c. Here the J/ψ decays radiatively by emission of two gluons.

The ratio of the partial widths of $J/\psi \to \gamma gg$ to $J/\psi \to ggg$, including first-order QCD corrections, is given by Brodsky et al. [83]

$$\frac{\Gamma(J/\psi \to \gamma gg)}{\Gamma(J/\psi \to ggg)} = \frac{36}{5} \frac{\alpha_{em}}{\alpha_s} q_c^2 \left[1 + (2.2 \pm 0.6) \frac{\alpha_s}{\pi}\right], \tag{4.2}$$

where α_{em} is Sommerfeld's fine structure constant and q_c the charmed quark charge. To evaluate this equation a value of $\alpha_s = 0.2$ will be used. It is obtained by calculating α_s in second order with a scale parameter of $\Lambda_{\overline{MS}} \simeq 100$ MeV. The result is $\Gamma(J/\psi \to \gamma gg)/\Gamma(J/\psi \to ggg) \simeq 13\%$. Correcting for the electromagnetic decays of the J/ψ gives a branching ratio prediction of $BR(J/\psi \to \gamma gg) \simeq 9\%$.

Experimental results on direct photon production from the J/ψ were obtained by the Lead-Glass-Wall [84] and Mark II [86] collaborations at SPEAR. Both experiments observe a branching ratio of about 4% for photon energies above 930 MeV, consistent with an expected 5% in this range. The photon energy spectrum from Mark II is shown in figure 7a. It is softer than that predicted in leading order calculations [87], but non-perturbative effects are expected to modify the high end of this spectrum [91].

It should be possible to describe radiative decays to exclusive final states by the same mechanism of γgg emission evaluated above. Therefore, we expect the QCD prediction to include the effects of resonances smeared over an appropriate mass region. Given the rather large γgg width, the production rate of mesons in radiative J/ψ decays should be sizable. A further step in this direction has been performed by Billoire et al. [92] and Körner et al. [93]. They carried out a spin-parity analysis of the produced two gluon system. The interesting feature is a strong presence of $J^{PC} = 0^{++}$, 0^{-+} and 2^{++} contributions (see fig. 7b). Predictions on the production of spin-one states depend crucially on the effective mass of the intermediate gluons as the formation of a vector particle by two massless gluons is forbidden by Yang's theorem [52]. Only massive gluons may produce such states.

One of the consequences of colored gluons interacting with each other is the possible existence of bound states of gluons [8], often referred to as gluonic mesons, gluonia or glueballs. Observation of such particles would provide a striking and very direct verification for the non-Abelian nature of QCD. The

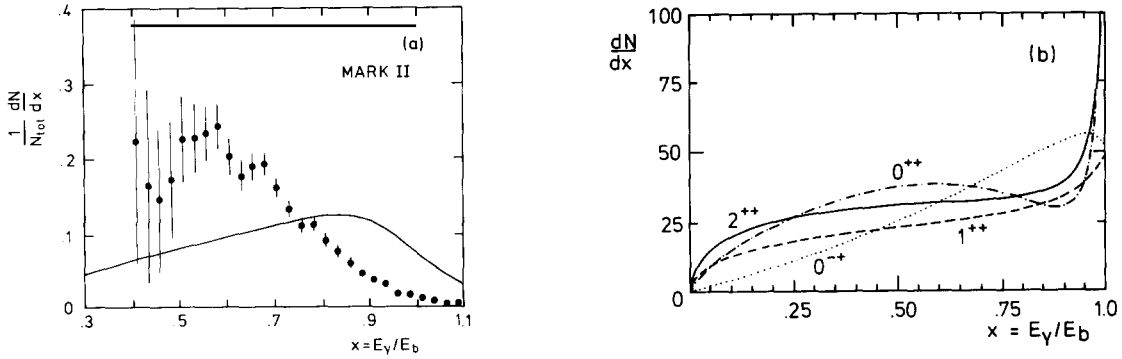

Fig. 7. (a) Mark II direct photon spectrum from the J/ψ. The solid curve is the leading order QCD prediction convoluted with the detector resolution; (b) the predicted photon spectrum for J/ψ radiative decays. Shown are the relative contributions to the spectrum from different spin-parities (from Körner et al. [93].

lightest gluonic mesons are expected to have masses ranging from 0.5–2.5 GeV and to have spin-parities 0^{++}, 0^{-+} and 2^{++}. This mass range is acessible in radiative J/ψ decays and these quantum numbers are expected to dominate this decay. In addition to gluonic and quark–antiquark meson production, it seems possible to form other states unknown in the quark model: the hybrid mesons $q\bar{q}g$ state [9] – also known as meiktons – and four-quark $q\bar{q}q\bar{q}$ states. All of those states should be produced strongly in the gluon rich channel $J/\psi \rightarrow \gamma gg$.

Unfortunately, QCD predictions on masses, widths and decay channels for gluonic, hybrid and four-quark structures are not very precise. This makes it difficult to distinguish these states from normal mesons. But some theoretical guidance is needed to help identify non-$q\bar{q}$ states. The models used to obtain predictions are lattice Monte Carlo calculations [94], bag models [95] and potential models [96].

The theoretical mass spectrum for gluonic mesons is shown in fig. 8. Indicated are typical predictions

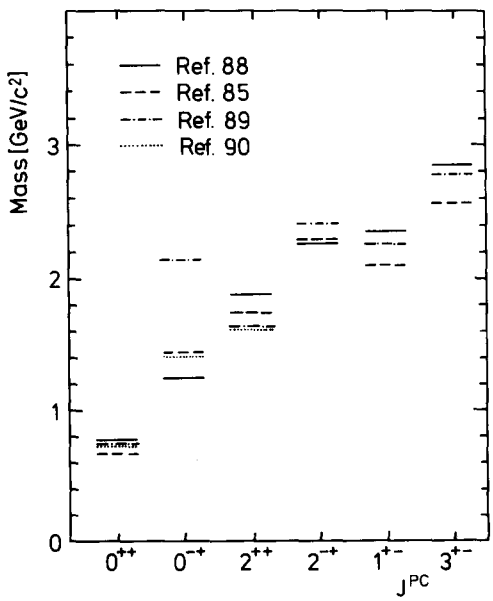

Fig. 8. The lowest-lying gluonic meson states for each of the indicated quantum numbers (from Carlson et al. [88]). Predictions are from bag models (lines without dots) and from lattice Monte Carlo calculations (lines with dots).

from bag models (lines without dots) and lattice calculations (lines with dots). The good agreement between both approaches is encouraging. As the mass region between 1 GeV and 2 GeV is also filled with normal $q\bar{q}$ mesons, additional information would be helpful. Early it has been speculated, that gluonic meson widths should be suppressed by $\sqrt{\Gamma_{OZI}\Gamma_{had}}$, where Γ_{OZI} is a typical OZI [97] decay width, such as $\phi \to 3\pi$. This rule would yield a width of about 1–10 MeV. Mixing with ordinary hadrons, however, will broaden gluonic mesons [98]. At present, a firm estimate on their width is not known.

A possible signature of gluonium might be its flavor-independent couplings, as such a meson is by nature an SU(3) flavor singlet. There are, however, various SU(3) breaking mechanisms. For instance, in the decay of a pseudoscalar gluonic meson, the decay rate turns out to be proportional to the final state (light) quark masses [99]. The conclusion is that, at present, there is only one solid criterion to distinguish a gluonic from a normal meson. A particle qualifies as a gluonic meson if it does not fit into any available meson nonet with the appropriate quantum numbers. For this reason it is very important to obtain as much information as possible on radiative decays to normal hadrons. Together with all the information on masses and decay widths will it be possible to ascertain the nature of any new object being found.

4.1. $J/\psi \to \gamma + \{\pi^0, \eta, \eta'\}$

The η and η' were among the first particles to be found in radiative decays of the J/ψ. The DASP [14] and DESY–Heidelberg [15, 100] collaborations found evidence for η and η' in the three-photon final state from the J/ψ. Later, the Mark II experiment [101] observed these mesons in their decay modes $\gamma\pi\pi$ and $\gamma\rho^0$, respectively. With the first large data set obtained by the Crystal Ball group, improved measurements on these decays became available. In particular the η' was seen in its decay modes $\eta\pi^+\pi^-$, $\eta\pi^0\pi^0$, $\gamma\rho^0$ and $\gamma\gamma$ [81] and the η in the mode $3\pi^0$ [60]. New information on η and η' has been added recently by the Mark III [102, 103] and DM2 [76] collaborations. The isopin forbidden decay of the J/ψ to $\gamma\pi^0$ has been determined by DASP [14], Crystal Ball [81] and DM2 [76]. The average branching ratios for the above discussed decay modes do not differ substantially from those listed in the Review of Particle Properties [59]. New average branching ratios have been calculated including recent measurements and are presented in table 10.

Average widths are calculated with $\Gamma(J/\psi) = 63$ keV and compared to three different theoretical calculations. The first prediction by Intemann [104] is based on an extended version of vector meson dominance. The decays into pseudoscalars P are assumed to proceed through all possible intermediate vector states V: $J/\psi \to VP \to \gamma P$. Fritsch and Jackson [105] introduce small admixtures of η and η' in the η_c wave function. The decay width to pseudoscalars is then calculated using the non-relativistic radiative

Table 10
Average branching ratios for $J/\psi \to \gamma + \{\pi^0, \eta, \eta'\}$. Experimental results are from refs. [59, 60, 76, 81, 101, 102, 103]. The experimental widths are calculated using $\Gamma(J/\psi) = 63$ keV, which introduces an additional 14% scale error. Three theoretical predictions are included

X	π^0	η	η'	Ref.
$BR(J/\psi \to \gamma X)(\times 10^3)$	0.038 ± 0.008	0.88 ± 0.06	3.9 ± 0.3	
$\Gamma(J/\psi \to \gamma X)$(eV)	2.4 ± 0.5	55 ± 4	246 ± 19	
Intemann	0.9 eV	69 eV	265 eV	[104]
Fritsch and Jackson	1 eV	60 eV	220 eV	[105]
Novikov et al.		79 eV	292 eV	[106]

decay formula (eq. (3.7)) multiplied by small mixing parameters. Novikov et al. [106] have used the parameter free approach of evaluating the QCD matrix element of the two-gluon field tensor between the vacuum and the η. The decay width to η′ is then calculated with QCD sum-rules. All predictions are very similar and agree well with experimental observations. The rather large decay width to γη′ points to a strong coupling of the η′ to gluons. In fact, an analysis of radiative decays of light pseudoscalar mesons [107] and an investigation of J/ψ decays to pseudoscalar-vector final states [79] suggests that a sizable gluon component may be present in the η′ wave function.

4.2. $J/\psi \to \gamma + \iota(1460)$

It has been argued in the introduction to this section, that the prime channel to look for gluonic and hybrid mesons is in radiative J/ψ decays. The first candidate, the ι(1460), was found by Mark II [108] in the decay mode $\iota \to K_s^0 K^{\pm}\pi^{\mp}$. The $K\bar{K}$ system is produced preferentially at low mass, as though the decay were $\iota \to \delta\pi$, $\delta \to K\bar{K}$. Without spin analysis the signal of about 85 events was tentatively identified with the $J^{PC} = 1^{++}$ E(1420) meson. Speculation on a gluonium hypothesis was nourished by the very large radiative branching ratio (see table 11).

Subsequently, the Crystal Ball studied the ι with greater statistics in the $K^+K^-\pi^0$ mode (174 ± 30 events). A partial wave analysis was performed [109] in 100 MeV bins of the $K\bar{K}\pi$ invariant mass. The decay was assumed to proceed through the two-body intermediate states δπ or K*K. Included were spin partities $J^P = 0^-$, 1^+, and three-body phase space. The result was a peak in the δπ ($J^P = 0^-$) channel. From the production mechanism C parity is established as even, thus $J^{PC}(\iota) = 0^{-+}$, different from the E(1420) meson. The decay into K*K was shown to be small (see table 11).

Table 11

Branching ratios for $J/\psi \to \gamma + \iota(1460)$. Isospin $I = 0$ has been assumed for the ι in order to calculate the total $K\bar{K}\pi$ branching ratio. If an experiment has measured the $K\bar{K}\pi$ final state in different charge combinations, the resulting mass values, widths and branching ratios have been averaged. All errors have been added in quadrature. Included is also the observed signal in $\gamma\rho^0$, which may be due to the ι. Upper limits are at the 90% confidence level.

	Mark II	Crystal Ball	Mark III	DM2
References	108	109, 110	102, 111	76
$\iota \to K_s^0 K^{\pm}\pi^{\mp}$ events	~85		340 ± 18	798 ± 36
$\iota \to K^+K^-\pi^0$ events		174 ± 30	402 ± 20	374 ± 46
Mass (MeV)	1440^{+10}_{-15}	1440^{+20}_{-15}	1459 ± 5	1456 ± 6
Γ (MeV)	50^{+30}_{-20}	55^{+20}_{-30}	99 ± 11	98 ± 13
for $M(K\bar{K})$	<1050	<1125	<1320	<1350
J^{PC}		0^{-+}	0^{-+}	0^{-+} consist.
$BR(J/\psi \to \gamma\iota, \iota \to K\bar{K}\pi) \times 10^3$	4.3 ± 1.7	4.0 ± 1.2	4.8 ± 0.6	4.1 ± 0.7
$\iota \to K^*K/(K^*K + \delta\pi, \delta \to K\bar{K})$		<0.25		
$\iota \to K^*K/K\bar{K}\pi$			<0.35	
$\iota \to \eta\pi\pi/K\bar{K}\pi$	<1.1	<0.5	<0.26	
$\iota \to (\delta\pi, \delta \to \eta\pi)/K\bar{K}\pi$			<0.14	
Mass in $\gamma\rho^0$ (MeV)		1390 ± 25	1420 ± 25	1401 ± 18
Γ (MeV)		185^{+110}_{-80}	133 ± 63	174 ± 44
$BR(J/\psi \to \gamma X, X \to \gamma\rho^0) \times 10^4$		1.9 ± 0.6	1.0 ± 0.3	0.9 ± 0.2

The Mark III [102] and DM2 [76] collaborations have measured (table 11) the ι(1460) with very high statistics; note that Mark III has also observed the ι in the decay channel $K_s^0 K_s^0 \pi^0$. Figure 9a shows the mass spectrum obtained by DM2 for the final state $J/\psi \to \gamma K_s^0 K^{\pm}\pi^{\mp}$. From the relative branching ratios to the final states $K_s^0 K^{\pm}\pi^{\mp}$ and $K^+K^-\pi^0$ both groups deduce that the isospin of the ι is consistent with $I = 0$, but it is impossible to rule out $I = 1$, $I_3 = 0$. The main changes with respect to the Mark II and Crystal Ball data are higher mass values and larger widths. This may be due to the low $K\bar{K}$ mass cut used in the first two observations. To test this hypothesis, the Mark III group imposed a mass cut of $M(K\bar{K}) < 1125$ MeV. A downward shift of (14 ± 7) MeV in mass and (10 ± 14) MeV in width was obtained. So this hypothesis does not fully explain the differences. Combining all experimental values on mass, width and branching ratio yields the average values

$$M_\iota = (1455 \pm 4)\,\text{MeV}\,, \qquad \Gamma_\iota = (89 \pm 8)\,\text{MeV}\,,$$

$$\text{BR}(J/\psi \to \iota) \times \text{BR}(\iota \to K\bar{K}\pi) + (4.4 \pm 0.4) \times 10^{-3}\,. \tag{4.3}$$

The Crystal Ball ι(1460) partial wave analysis suffered from two complications: (a) limited phase space causes the δπ and K*K events to overlap in much of the Dalitz plot, and (b) the properties of the δ(980) are poorly understood. Therefore, Mark III and DM2 have both reanalyzed the spin parity of the ι using the three-body helicity formalism of Berman and Jacob [112]. This determines the ι spin completely independent of the Dalitz plot structure. They find consistency with $J^P = 0^-$; Mark III determines relative likelihoods for $\mathscr{L}(1^{\pm})/\mathscr{L}(0^-)$ to less than 3×10^{-4}. A spin 2 assignment has not yet been tested for and, although such a high spin seems unlikely in this mass region, it cannot be ruled out. From an analysis of the $K\bar{K}\pi$ Dalitz plot Mark III obtains an upper limit on the ι decay into K*K of less than 35% (table 11).

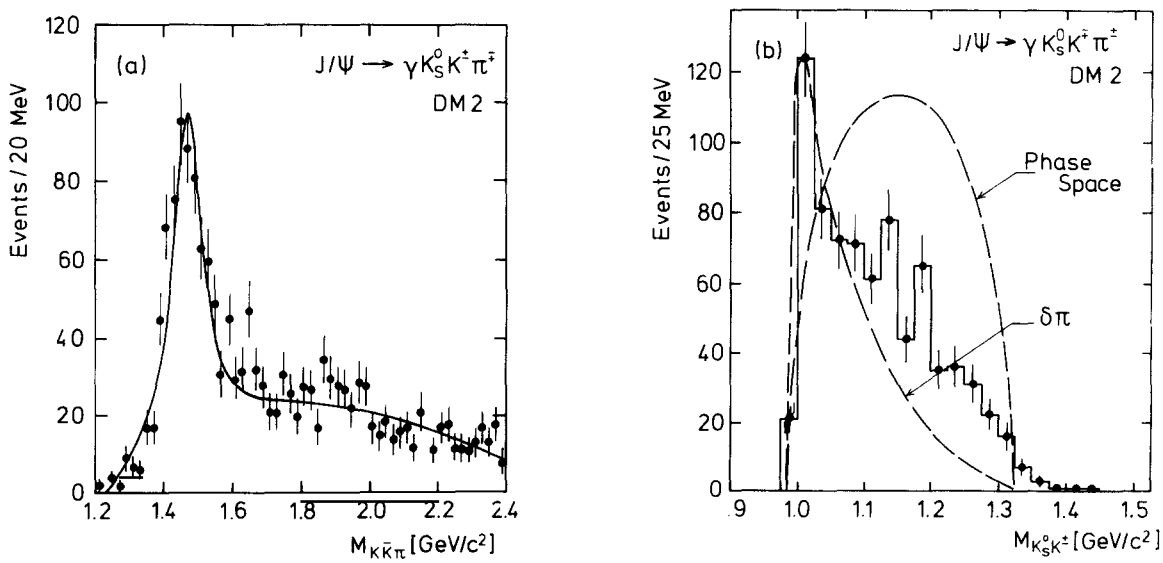

Fig. 9. DM2 results on $J/\psi \to \gamma K_s^0 K^{\pm}\pi^{\mp}$: (a) the invariant mass $M(K_s^0 K^{\pm}\pi^{\mp})$; (b) $M(K_s^0 K^{\pm})$ for $1.3\,\text{GeV} < M(K_s^0 K^{\pm}\pi^{\mp}) < 1.6\,\text{GeV}$ with projections from δπ and $K\bar{K}\pi$ phase space.

4.2.1. Theoretical Explanations

The observed enhancement in $M_{K\bar{K}}$ towards low masses (see fig. 9b) has been explained from the very beginning as an indication of an intermediate state, the δ(980). The δ, along with its partner the S*(975), have been known for a long time. Their natural assignments are the isospin triplet and singlet states of the $1\,^3P_0$ nonet with $J^{PC} = 0^{++}$, but there are some severe problems with this interpretation (see, e.g., Review of Particle Data Properties [59]). The width of the δ is much narrower than expected, which may be due to its mass being below $K\bar{K}$ threshold. Branching ratios have been notoriously difficult to measure. Accepted values [59] are $BR(\delta \to K\bar{K})/BR(\delta \to \eta\pi) = 0.25 - 4.2$. Given this range of branching ratios, the ι should also decay to ηππ with at least one-quarter the strength of the $K\bar{K}\pi$ decay mode. These decays have been searched for, see table 11 and fig. 10. The upper limit from Mark III on the ratio of branching ratios $BR(\iota \to \delta\pi, \delta \to \eta\pi)/BR(\iota \to K\bar{K}\pi)$ of 0.14 is stringent enough to make one wonder what other mechanism inhibits the ηππ decay mode.

Several solutions for this problem have been suggested. Jaffe [113] had shown that the δ can be explained as a four-quark state. Following this idea, Frank et al. [114] interpret the δ as a $K\bar{K}$ molecule. Here the low mass enhancement in $K\bar{K}$ was shown to arise from a distortion of the $K\bar{K}\pi$ final state. Palmer et al. [115] suggest interference effects to be responsible for the observed absence of the ηππ decay mode. They require destructive interference between the two competing ι decay channels $\iota \to \delta\pi$ and $\iota \to \eta\epsilon$, where ε stands for the elusive isospin 0, $J^{PC} = 0^{++}$ ππ resonance at about 700 MeV. They predict for the ηππ decay as little as 10% of the rate for KKπ, comfortably below experimental observation. Both of the above ι decay analyses show that a gluonium interpretation is possible.

In the mass region around 1400 MeV another particle exists that decays to $K\bar{K}\pi$, the E(1420). The E and ι are considered different states due to their different spin-parities and their slightly different masses and widths:

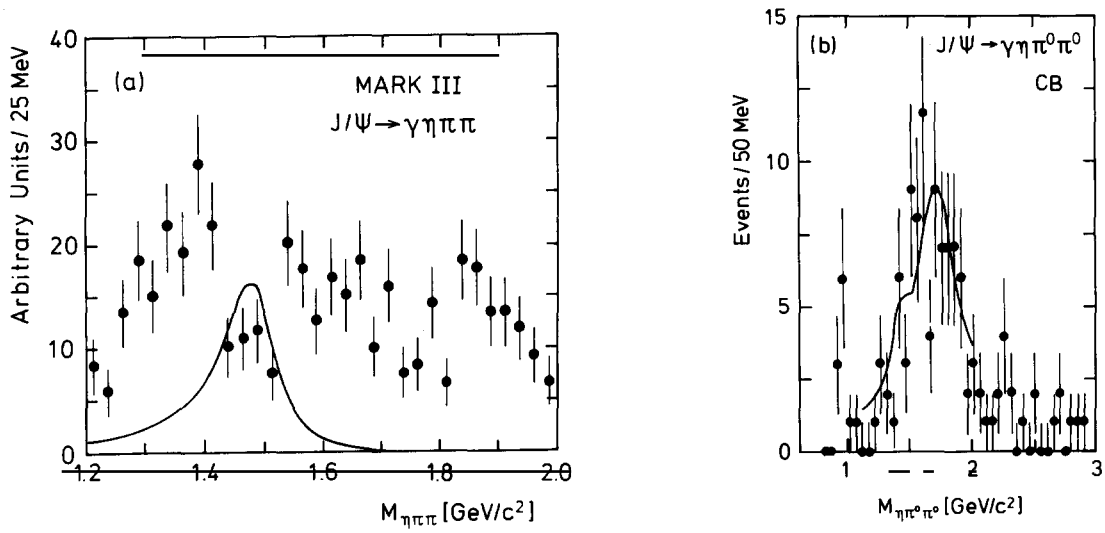

Fig. 10. (a) Mark III $J/\psi \to \gamma\eta\pi^+\pi^-$ [102] corrected for efficiency (arbitrary units). A cut on the ηπ mass around the δ has been applied. The curve is used to calculate an upper limit on ι production. (b) Crystal Ball $J/\psi \to \gamma\eta\pi^0\pi^0$ [110]. The fit to the broad structure at about 1700 MeV includes a possible contribution from the ι.

$$M_\iota = (1455 \pm 4)\ \text{MeV}, \quad \Gamma_\iota = (89 \pm 8)\ \text{MeV}, \quad J^{PC} = 0^{-+}, \qquad (4.4)$$
$$M_E = (1418 \pm 4)\ \text{MeV}, \quad \Gamma_E = (52 \pm 5)\ \text{MeV}, \quad J^{PC} = 1^{++}.$$

The E was first discovered by Baillon et al. [116] in $p\bar{p}$ annihilations at rest. A spin-parity analysis led to $J^{PC} = 0^{-+}$, compatible with the ι. Later $\pi^{\pm}p$ experiments [117, 118], however, assigned 1^{++} to the E. Very recent $\pi^- p$ experiments [119, 120] again reversed the spin-parity to 0^{-+}. Note that the experiment by Ando et al. [120] has also observed the E in the final state $\eta\pi\pi$. A big difference shows up in the analysis of intermediate two-particle states in $K\bar{K}\pi$. Experiments which observe the E as $J^{PC} = 1^{++}$ seem to find a dominant decay via K*K; for a 0^{-+} E the intermediate state mostly resonates in $\delta\pi$, as is also found for the ι. Except Baillon et al. all experiments observe the D(1275), a $J^{PC} = 1^{++}$ state, in their $K\bar{K}\pi$ data. For a detailed discussion of the E in hadronic reactions see the review by Cooper [121].

Concluding this excursion into the realm of hadronic production of pseudoscalar and vector mesons, it seems that three particles exist in the mass region around 1400 MeV. The E(1420) with spin-parity 1^{++} decaying to K*K, another state at 1420 MeV with 0^{-+} decays to $\delta\pi$, and the ι(1460) with $J^{PC} = 0^{-+}$ which also decays to $\delta\pi$. The 1^{++} E can be accommodated in the ground state $^3P_1$ nonet, but the mixing angle required is rather large with 47° (Montanet [122]). But note that a mixing analysis in this channel is complicated due to additional mixing between the strange mesons $Q_1(1280)$ and $Q_2(1400)$ of the 1^{++} and 1^{+-} nonets. Potential and quark models place the E mass around 1400 MeV, see e.g. Bander et al.[123] and Törnqvist [124]. Assuming the mixing angle to be close to ideal ($\theta \simeq 35°$), another possible, unconfirmed state, the D′(1526) [125], would fit into this nonet better than the E. With this assignment the 1^{++} E would be required to belong to the first radial excitation, but for that its mass seems too low. Altogether, the question on the E has not been solved yet, and more data are definitely needed to find its right assignment.

The question arises whether the 0^{-+} X(1420) and ι are in fact the same particle. Whereas X(1420) mass and width determined in hadronic collision experiments are all very similar, the ι seen by Mark III and DM2 in radiative decays has a higher mass and a larger width. Given this mass and width difference and the fact that X(1420) has been seen in $\eta\pi\pi$, it seems that both are different states. The interpretation of X(1420) as a radially excited pseudoscalar state together with the η(1275) [120, 126] fails due to the small mass of the X(1420) [127]. But if a gluonic meson exists somewhere in this mass range, the result will be strong mixing and a shift of the bare masses. The 0^{-+} ι(1460) is a good gluonic meson candidate, although an interpretation as a radially excited pseudoscalar also seems possible [128].

How well does the ι(1460) fit a gluonic meson interpretation? The mass of a $J^{PC} = 0^{-+}$ gluonium state is expected in the vicinity of 1400 MeV, see fig. 8, from such different approaches as bag models [85, 88], lattice gauge calculations [89–90], potential models [96] and massive constituent gluon models [129]. The width of a gluonic meson was initially argued to be approximately few MeV, but some calculations [130, 131] can explain a large width of 50 MeV. The ι production rate in radiative J/ψ decays is larger than that to the lowest lying pseudoscalars η and η′, as expected for a state rich in gluons. The observed dominance of $\delta\pi$ and the absence of $\eta\pi\pi$ can be explained [114, 115]. Mixing with (bare) $q\bar{q}$ pseudoscalar states has been taken into account [98, 107, 132], but conclusions on such mixing are not unanimous.

4.2.2. ι(1460)→γρ⁰

Additional information on the nature of the ι may be provided by its electromagnetic decays. For a gluonic meson one expects these decays to be suppressed as gluons do not couple to photons. Such a transition is possible only through intermediate $q\bar{q}$ states. The decay $\iota \to \gamma\rho^0$ has been suggested very early

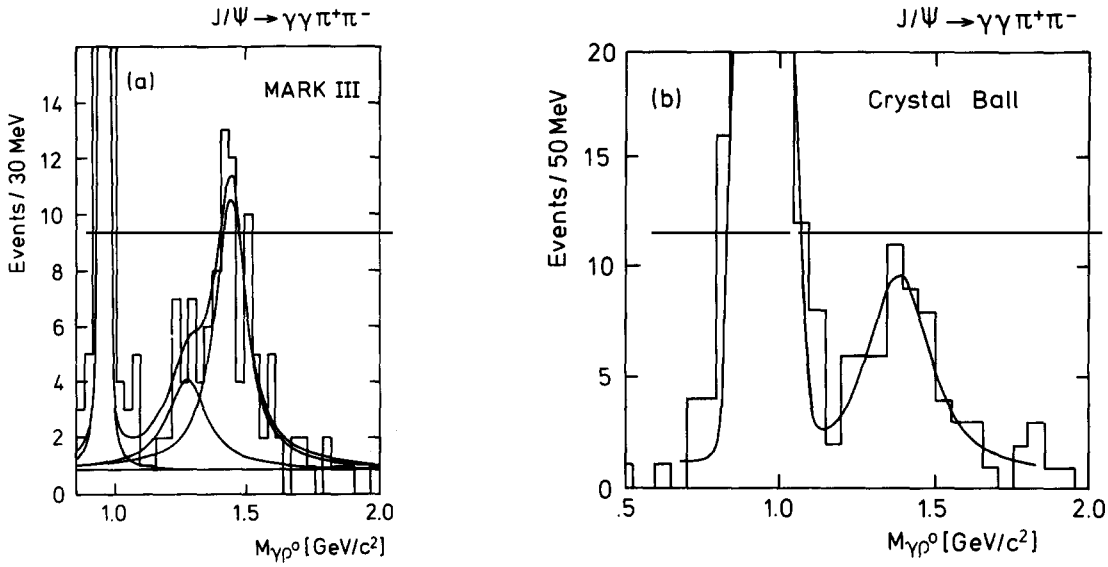

Fig. 11. Invariant $\gamma\rho^0$ mass distribution from $J/\psi \to \gamma\gamma\pi^+\pi^-$, (a) Mark III, the fit includes contributions from η', $\eta(1275)$ and X(1434); (b) Crystal Ball, with fit to η' and X(1390).

as an additional test of the ι constituents. The predicted widths [133, 134] range from about 0.4 MeV to 4 MeV. However, a radially excited $q\bar{q}$ state, the other possible assignment for the ι(1460), also has a small radiative decay width of about 0.2 MeV. Assuming the ι to decay mainly into $K\bar{K}\pi$ a width of 2 MeV would correspond to a sizable branching fraction $BR(J/\psi \to \gamma\iota, \iota \to \gamma\rho^0) = 2 \times 10^{-4}$.

DM2 [76], Crystal Ball [135] and Mark III [102] have reported a peak in $\gamma\rho^0$ around 1.4 GeV, see table 11. Figure 11 shows the spectra obtained by Crystal Ball and Mark III. The observed enhancement is about $1\text{–}2\sigma$ lower in mass and has a width larger than the ι observed in $K\bar{K}\pi$. It is conceivable [102, 135], that more than one resonance contribute to the signal or that background populates the low-mass side of the peak. With these difficulties in mind, Mark III has fit the spectrum with three resonances: the η', $\eta(1275)$ and a state X to be determined by the fit. A mass of X(1434) resulted, see fig. 11a. All experiments find a branching ratio of $BR(J/\psi \to \gamma X, X \to \gamma\rho^0) \simeq (1-2) \times 10^{-4}$, consistent with the range of theoretical predictions stated above. Thus the $\gamma\rho^0$ signal is compatible with a gluonium interpretation of the ι if a low mass contribution from another channel is taken into account. The $\gamma\rho^0$ signal is also compatible with the structure near 1380 MeV observed in the $\eta\pi\pi$ channel (see fig. 10). An analysis of the $\gamma\rho^0$ decay angular distributions agrees with the prediction for spin-parity 0^-, but higher spins cannot be ruled out. With the present statistics, it is not possible to unambiguously identify the peak in fig. 11 as being due to the ι(1460).

5. Radiative decays to two vector mesons

Enhancements in ρρ final states below masses of 2 GeV were found in hadronic interactions [136] and in photon–photon collisions [137], for a review see Kolanoski, ref. [138]. In addition, φφ resonances were observed [139] near 2.2 GeV in π^-p interactions. Interpretations of the φφ enhancements include bound states of normal $q\bar{q}$ mesons, four-quark $q\bar{q}q\bar{q}$ states, hybrid $q\bar{q}g$ and gluonic mesons gg (see Lindenbaum [140]).

5.1. $J/\psi \to \gamma + \rho\rho$

The decay $J/\psi \to \gamma\rho^0\rho^0$ was first observed by Mark II [141]. The $\rho^0\rho^0$ mass distribution is dominated by a structure around a mass of 1.65 GeV. At first it was believed that this structure might be associated with the $\Theta(1700)$, to be discussed in section 6.3. The Mark III group has analyzed [142] the two modes $\pi^+\pi^-\pi^+\pi^-$ and $\pi^+\pi^0\pi^-\pi^0$. Both channels show similar 4π invariant mass distributions. The summed mass spectrum is shown in fig. 12a. Two peaks at ~1.55 GeV and ~1.8 GeV are the striking feature. The background is mostly due to non-resonant $J/\psi \to 5\pi$ and can easily be subtracted. The Crystal Ball analyzed the mode $\pi^+\pi^0\pi^-\pi^0$ [135] and found a broad single peak around 1.7 GeV. The total $\rho\rho$ branching ratio below 2 GeV is substantial:

$$BR(J/\psi \to \gamma\rho^0\rho^0) = (1.3 \pm 0.5) \times 10^{-3} \quad \text{for} \quad M_{\rho\rho} < 2.0\,\text{GeV} \qquad \text{Mark II},$$

$$BR(J/\psi \to \gamma\rho^+\rho^-) = (3.1 \pm 1.1) \times 10^{-3} \quad \text{for} \quad M_{\rho\rho} < 1.9\,\text{GeV} \qquad \text{Crystal Ball}.$$

The ratio of branching ratios $BR(\rho^+\rho^-)/BR(\rho^0\rho^0) = 2.4 \pm 1.2$ is consistent with a value of 2 expected for an isoscalar $\rho\rho$ system.

The spin-parity of the $\rho\rho$ system was examined using two different approaches. Mark III and Crystal Ball performed an analysis of the angle between the two $\rho \to \pi\pi$ decay planes in the $\rho\rho$ center-of-mass frame. For the structure below 2 GeV clear evidence resulted for even spin and odd parity. This rules out the identification of this structure with the $\Theta(1700)$.

In a multichannel spin-parity analysis Mark III [142] found a large pseudoscalar $\rho\rho$ component for masses less than 2 GeV, shown in fig. 12b. They obtained a total branching ratio of

$$BR(J/\psi \to \gamma X_{0^-}) \times BR(X_{0^-} \to \rho\rho) = (4.7 \pm 1.0) \times 10^{-3}$$

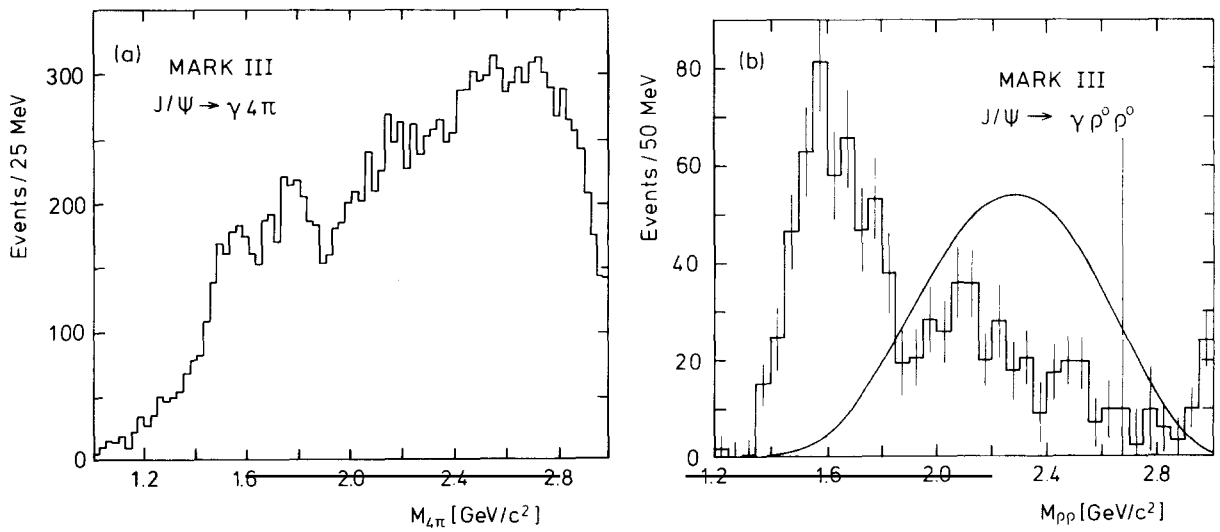

Fig. 12. Mark III invariant 4π mass spectrum in $J/\psi \to \gamma 4\pi$ decays: (a) shows the sum of both charge combinations; (b) the 0^- $\rho\rho$ component. The curve represents P-wave phase space.

for the 0^- ρρ component. The mass distribution in fig. 12b does not exhibit the two-peak structure seen in the full spectrum. But the uncertainties introduced by an analysis of this type prevent a definite identification with one or both structures seen in the 4π invariant mass distribution. The 0^- ρρ mass distribution is inconsistent with non-resonant P-wave ρρ production. The ratio between the data and phase space prediction is largest in the (1.4–1.5) GeV region, supporting an interpretation of $\iota \to \rho\rho$ decay distorted by phase space and P-wave factors. This will be described in more detail at the end of this chapter.

5.2. $J/\psi \to \gamma + \{\omega\omega, \phi\phi\}$

Both, Mark III [143] and DM2 [76] have observed $J/\psi \to \gamma\omega\omega$. Figure 13 shows the ωω invariant mass distribution obtained by Mark III. The shaded band displays the background contribution. For ωω masses less than 2.0(2.8) GeV Mark III (DM2) obtained branching ratios

$$\mathrm{BR}(J/\psi \to \gamma\omega\omega) = (1.2 \pm 0.3) \times 10^{-3} \quad \text{for} \quad M_{\omega\omega} < 2.0\,\mathrm{GeV} \qquad \text{Mark III},$$

$$\mathrm{BR}(J/\psi \to \gamma\omega\omega) = (0.8 \pm 0.2) \times 10^{-3} \quad \text{for} \quad M_{\omega\omega} < 2.8\,\mathrm{GeV} \quad \text{DM2}.$$

Both groups performed an analysis of the angle between the two ω decay planes. Below a mass of 2 GeV they find a large component with even spin and odd parity. A multichannel analysis by Mark III [143] yields clear evidence for 0^- spin-parity in this mass region.

Finally, the decay $J/\psi \to \gamma\phi\phi$ has been investigated. Here the φ is detected in its K^+K^- decay mode. The φφ state is of particular interest as the g_T states [140] were discovered in this channel in π^-p scattering experiments. DM2 applied a loose time-of-flight (TOF) cut to enhance the detection efficiency (fig. 14b) at low masses. The result in fig. 14a shows a substantial φφ signal. No background was found that could contribute to the signal. For φφ masses less than 2.8 GeV they determined a branching ratio of

$$\mathrm{BR}(J/\psi \to \gamma\phi\phi) = (3.1 \pm 0.7) \times 10^{-4}.$$

As a spin-parity analysis of this system has not yet been performed, no conclusions can be drawn with regard to the g_T resonances.

5.3. *The pseudoscalar puzzle*

The term 'pseudoscalar puzzle', coined by Wermes [144], refers to the existence of at least three pseudoscalar states below 2 GeV seen in radiative J/ψ decays. They are the $\iota(1460) \to K\bar{K}\pi$ and the ρρ, ωω and maybe the $\gamma\rho^0$ enhancements. In addition, a large radiative rate to ηππ suggests the existence of at least one other state in this mass region, but its spin-parity has yet to be measured. The obvious question arises whether all these enhancements are indeed new states or whether they originate from the same particle, a strong candidate being the ι(1460).

Based on a preliminary version of the Mark III results described above, Achasov et al. [145] have suggested that the pseudoscalar ρρ and ωω component can be accounted for by the ι(1460) interfering with the tail of the η′ and distorted by phase space and P-wave factors. Mark III has performed a coupled channel analysis of ι(1460) decays to $K\bar{K}\pi$, ρρ, ωω and $\gamma\rho^0$, including unitarity and threshold effects. The fit results [144] are shown as curves superimposed on the data in fig. 15.

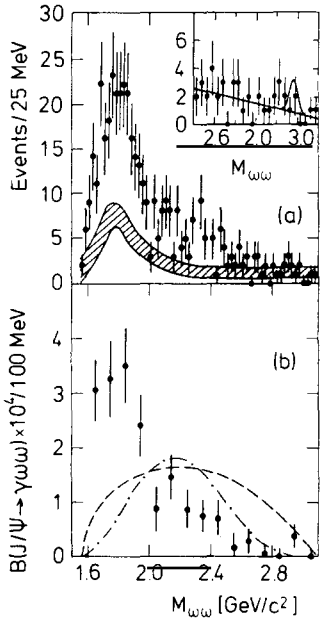

Fig. 13. (a) Mark III invariant ωω mass spectrum from $J/\psi \to \gamma\omega\omega$. The band represents the background contribution. The mass region around the η_c is shown in the inset. (b) BR($J/\psi \to \gamma\omega\omega$) in 100 MeV bins. The curves represent S-wave (dashed) and P-wave (dashed-dotted) phase space.

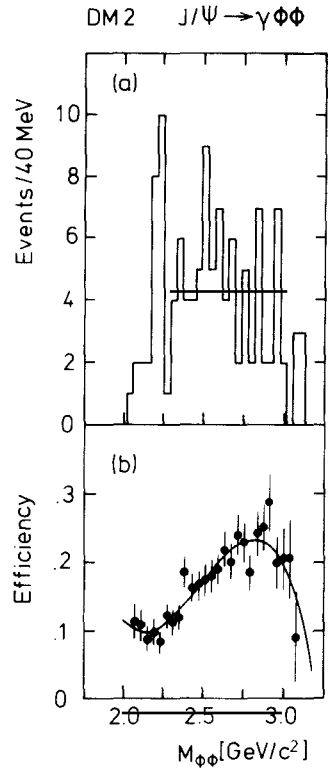

Fig. 14. (a) DM2 invariant φφ mass spectrum from $J/\psi \to \gamma\phi\phi$; (b) detection efficiency.

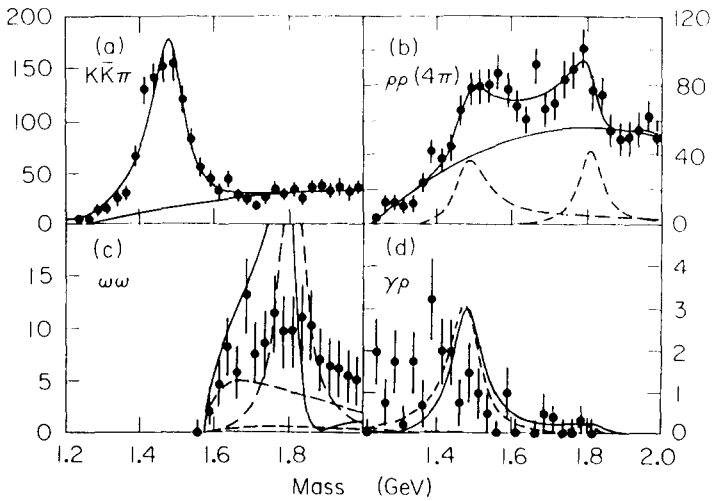

Fig. 15. Mark III coupled channel fit for (a) $K\bar{K}\pi$, (b) ρρ with background subtracted, (c) ωω with background subtracted, and (d) $\gamma\rho^0$ with background subtracted. The solid curves represent the total result of the fit plus background, the dashed curves indicate resonance contributions from ι(1460) and an assumed state at ~1800 MeV.

The coupled channel fit shows that the lower part of the ρρ mass distribution can be explained by a resonance below threshold, the ι(1460). Another resonance X(1800) had to be included to describe the full spectrum. This state is assumed not to couple to $K\bar{K}\pi$. The ωω mass distribution is also well described by the fit. Here strong interference between ι and X modifies the fit substantially. SU(3) predicts the coupling to ρρ to be three times that to ωω, the fit yields 5.0 ± 0.7, in reasonable agreement. The shape of the $\gamma\rho^0$ spectrum is not well reproduced. As phase-space effects are negligible in this channel, the peak of the Breit–Wigner should appear at the position of the ι(1460). Contributions from η(1275) might be responsible for the lower mass part of the $\gamma\rho^0$ signal, but this possibility has not been included in the fit. Vector dominance predicts a ratio of 400 for the ρρ to $\gamma\rho^0$ coupling, the fit yields 3300 ± 600. This is indicative of an additional resonance contributing to the signal.

Based on the coupled channel analysis, the following branching ratios have been determined:

$$\mathrm{BR}(J/\psi \to \gamma\iota) \times \mathrm{BR}(\iota \to \rho\rho) \simeq (1.5 \pm 0.2) \times 10^{-3},$$

$$\mathrm{BR}(J/\psi \to \gamma\iota) \times \mathrm{BR}(\iota \to \omega\omega) \simeq (0.3 \pm 0.1) \times 10^{-3},$$

$$\mathrm{BR}(J/\psi \to \gamma X(1800)) \times \mathrm{BR}(X(1800) \to \rho\rho) \simeq (1.0 \pm 0.2) \times 10^{-3}.$$

Including the decay to $K\bar{K}\pi$ the total known branching fraction to γι(1460) amounts to

$$\mathrm{BR}(J/\psi \to \gamma\iota) = (6.3 \pm 0.5) \times 10^{-3},$$

the largest radiative rate observed in J/ψ decays to non-charmonium states. The ηππ mass distribution (fig. 10a) was also tested for the hypothesis ι(1460) origin. It was found that this spectrum cannot accommodate the ι. Nor can the peak at 1380 MeV in ηππ be responsible for the structures observed in the other spectra in fig. 15. At the time being ηππ has to be left out of the pseudoscalar analysis. New insights into this puzzle may be expected because DM2 has not yet performed a coupled channel analysis and Mark III has not included the data taken in 1985.

The ι(1460) is certainly one of the most exciting results found in J/ψ decays. It is the oldest of the gluonic meson candidates, and yet the present experimental situation is still confusing. With the confirmation of the η(1275) [120, 126] it is hard to understand the mass pattern and production rates in $J/\psi \to \gamma\{\iota, \eta(1275)\}$ if both particles are the isoscalar states in the radially excited pseudoscalar $q\bar{q}$ nonet. It seems that the ι(1460) would have to be a gluonic meson or at least have a substantial gluon content.

6. Radiative decays to tensor particles

It was shown in the introduction to chapter 4, that the two gluon system produced in radiative decays contains a substantial $J^{PC} = 2^{++}$ component (see fig. 7b). Thus the radiative decay to the tensor mesons f(1270) and f'(1525) should proceed with a large rate, comparable to the decay $J/\psi \to \gamma\eta'$. A contrasting estimate on the strength of $J/\psi \to \gamma f$ can be obtained using vector dominance. Comparison with the measured rate $J/\psi \to \omega f$ of $(0.23 \pm 0.08)\%$ results in a γf decay rate similar to the very small $\gamma\pi^0$ mode. The assumption that radiative decays proceed through a small $c\bar{c}$ component in the final-state meson wave function also yields a very small rate, because the f is not expected to have an appreciable $c\bar{c}$ component. To test these different assumptions, it is important to measure the strength of radiative transitions to

tensor mesons. In addition, the appearance of unexpected tensor states may provide new information on the existence of exotic particles.

The f(1270) and f′(1525) are the two iso-singlet members of the lowest lying 2^{++} $q\bar{q}$ nonet. This nonet is observed to be nearly ideally mixed, i.e. the f(1270) is almost pure $u\bar{u} + d\bar{d}$ and the f′(1525) is pure $s\bar{s}$. Therefore a search for these states in radiative J/ψ decays concentrates on the decay modes $f \to \pi\pi$ and $f' \to K\bar{K}$. This section starts with a discussion of the experimental results on the f(1270) and f′(1525) and assesses the mixing situation. A summary of the experimental information on a new state, the Θ(1700), follows. An evaluation of its possible interpretations is given.

6.1. $J/\psi \to \gamma + f(1270)$

The DASP [14] and PLUTO [146] groups at DESY were the first experiments to observe the f(1270) in radiative J/ψ decays. Later, the Mark II [147] detector also measured this decay. All experiments used the charged decay mode $f \to \pi^+\pi^-$. Here a problem arises from the feed-through of $J/\psi \to \pi^0\rho^0$, $\rho^0 \to \pi^+\pi^-$ events with one undetected photon. The Crystal Ball [148] has studied the decay mode $f \to \pi^0\pi^0$ which is free of this background. Based on much larger J/ψ data samples, Mark III [103] and DM2 [76] have determined very precise branching ratios. The latter group has analyzed both the charged and neutral pion decay modes of the f.

Figure 16 shows the spectra obtained by Mark III [103] and Crystal Ball [60]. The similarity between both spectra is striking, although different final states $\pi^+\pi^-$ and $\pi^0\pi^0$ were analyzed. At a mass of about 1270 MeV is the large signal due to the f. Averaging all experimental branching ratios, mass and width determinations yield [14, 76, 103, 146, 148]

$$\begin{aligned} &\mathrm{BR}(J/\psi \to \gamma f) = (1.35 \pm 0.11) \times 10^{-3}\,, \\ &M_f = (1262 \pm 4)\ \mathrm{MeV}\,, \qquad \Gamma_f = (200 \pm 7)\ \mathrm{MeV}\,, \end{aligned} \tag{6.1}$$

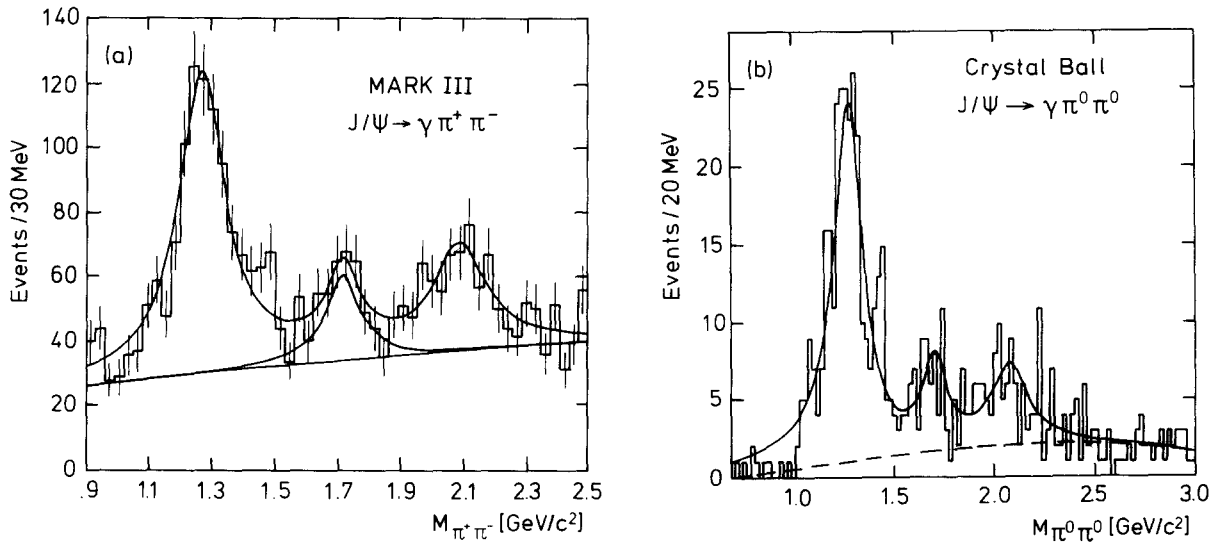

Fig. 16. Invariant ππ mass distributions from (a) Mark III $J/\psi \to \gamma\pi^+\pi^-$ and (b) Crystal Ball $J/\psi \to \gamma\pi^0\pi^0$. The solid curves represent a fit with three non-interfering Breit–Wigner line shapes and a smooth background (phase space in (b)). In (a) the widths for the first and second peak are fixed. In (b) the mean and width for the second and third peak are fixed to the values found by Mark III.

where statistical and systematic errors have been added in quadrature. The average mass and width from all experiments are not inconsistent with the values stated in ref. [59]: $M_f = (1274 \pm 5)$ MeV and $\Gamma_f = (178 \pm 20)$ MeV. QCD γgg decay analyses yield predictions for the branching ratio [93, 149] in good agreement with data.

All four experiments Mark II, Crystal Ball, Mark III and DM2 find a structure on the high mass side of the f(1270), see fig. 16. Although the significance in each individual experiment is small, the combined evidence seems considerable. A source for this structure could be the decay $f'(1525) \to \pi\pi$. This hypothesis has been tested [103, 76]. The corresponding branching ratio $f' \to \pi\pi$ depends strongly on a possible interference between the f and the second peak, but is consistent with expectation [76]. No such structure is seen in $J/\psi \to \omega\pi^+\pi^-$ [103, 76], consistent with OZI suppression of $J/\psi \to \omega f'$. Note that this structure in the Crystal Ball data is at a mass of ~1450 MeV, a little too low to be associated with the f'(1525). With the presently analyzed data it seems impossible to achieve a better understanding of this structure.

The spectra contain indications for the presence of additional structures above the f(1270). The interpretation of these structures is ambiguous. A fit with three Breit–Wigners added incoherently gives the best description [103]. Here the widths of the f and the second peak have been fixed at 180 MeV and 130 MeV, the latter corresponding to the width of the Θ(1700) seen in the decay mode K^+K^- (see section 6.3).

These high mass structures can be interpreted in terms of Θ(1700) and an additional resonance with a mass of about 2 GeV. For the Θ candidate, the observed mass, width and angular distribution of the pion in the ππ center-of-mass system are quite consistent [103] with those observed in the K^+K^- channel. No clear interpretation exists for the higher mass state, but it could be an orbitally excited f, possibly the h(2030). Averaged results from Mark III and DM2 on the high mass peak yield [76, 103]

$$\begin{aligned} &\mathrm{BR}(J/\psi \to \gamma X,\ X \to \pi^+\pi^-) = (3.5 \pm 0.6) \times 10^{-4}\,, \\ &M_X = (2065 \pm 30)\ \mathrm{MeV}\,, \qquad \Gamma_X = (293 \pm 40)\ \mathrm{MeV}\,, \end{aligned} \tag{6.2}$$

where the errors on the mass and width have been increased by $\sqrt{\chi^2}$ as the individual errors do not cover the range of the two measurements. The results are consistent with those of the h(2030) meson $M_h = (2027) \pm 12)$ MeV and $\Gamma_h = (220 \pm 30)$ MeV [59].

The spin of a resonance observed in J/ψ radiative decays can be determined from an analysis of the angular distributions of the detected particles. For a particle of spin-parity 2^+, three complex helicity amplitudes describe the decay distributions, corresponding to helicity 0, 1 and 2 of the state. By taking ratios, this number is reduced to four real quantities $(x, \phi_x; y, \phi_y)$, defined by

$$A_1/A_0 = x \exp i\phi_x\,, \qquad A_2/A_0 = y \exp i\phi_y\,. \tag{6.3}$$

The helicity amplitude ratios and their phases are then determined by a fit to the decay angular distribution given by Kabir and Hey [150].

For the f(1270), such analyses have been performed by PLUTO [146], Mark II [147], Crystal Ball [148] and Mark III [103] using χ^2 or maximum likelihood fits. The results obtained are listed in table 12. The first three analyses considered only real helicity amplitudes, i.e., phases were fixed at zero. Mark III finally has shown that the phases are actually very close to zero, validating the earlier approaches. All measurements yield $x \simeq 0.9$ and $y \simeq 0$.

Table 12
Summary of polarization measurements for f(1270), f'(1525), and Θ(1700). Phases were either fixed (0, 0) or were found to be consistent with zero (~0, ~0). Included are two theoretical predictions assuming pure quark [93] and pure gluonic structure [152]. For electric dipole transitions $(x, y) = (\sqrt{3}, \sqrt{6})$.

	Ref.	PLUTO [146]	Mark II [147]	Crystal Ball [148]	Mark III [103]	DM2 [76]	Körner [93]	Li, Shen [152]
f	x	0.6 ± 0.3	0.8 ± 0.2	0.9 ± 0.1	1.0 ± 0.1		0.77	0.66
	y	$0.3^{+0.6}_{-1.6}$	0.0 ± 0.2	0.0 ± 0.1	0.1 ± 0.1		0.55	0.04
	(ϕ_x, ϕ_y)	(0, 0) fixed	(0, 0) fixed	(0, 0) fixed	(~0, ~0)		(2°, 4°)	
f'	x				0.6 ± 0.1	1.1 ± 0.1	0.90	
	y				$0.2 \pm 0.2)$	0.2 ± 0.1	0.72	
	(ϕ_x, ϕ_y)				(~0, ~0)	(~0, ~0)	(1.3°, 2.4°)	
Θ	x		1.2 ± 0.6	0.9 ± 0.2	-1.1 ± 0.2	-1.3 ± 0.1	0.96	
	y		-0.9 ± 0.6	-0.6 ± 0.4	-1.1 ± 0.3	-1.1 ± 0.2	0.81	
	(ϕ_x, ϕ_y)		(0, 0) fixed	(0, 0) fixed	(~0, ~0)	(~0, ~0)	(1.1°, 1.8°)	

The helicity amplitude ratios can be estimated for two limiting cases. In the case of electric dipole radiation ($kr \ll 1$) we obtain $(x, y) \rightarrow (\sqrt{3}, \sqrt{6})$. On the other hand, if the f mass were negligible with respect to $M_{J/\psi}$, then the f would be produced in a zero helicity state: $(x, y) \rightarrow (0, 0)$. Experimental data show that none of these two cases are applicable. Körner et al. [93] calculate the helicity ratios in lowest order QCD assuming the decay to proceed through emission of a photon and two gluons. They find the helicity ratios to depend only on $m_f/M_{J/\psi}$ and to be rather similar to each other (see table 12). Thus, in order to explain the data, one would need some other mechanism to suppress the helicity 2 amplitude. Maybe the low experimental y value is indicative of a dynamical selection rule [151]. Assuming a gluonium hypothesis for the f, Li and Shen [152] have calculated the helicity ratios. The agreement between data and theory is striking. Unfortunately, their proposal would require both the f(1270) and f'(1525) to be gluonic mesons, an assumption which does not seem reasonable. Indeed, it has been shown [153] that neither of those two states require a gg component.

6.2. $J/\psi \rightarrow \gamma + f'(1525)$

The natural place to search for the f'(1525) is in the decay mode $f' \rightarrow K\bar{K}$. In radiative J/ψ decays the f' was first observed by Mark II [154] and later firmly established with the big data samples of the Mark III and DM2 detectors. Both experiments have found the f'(1525) in the channels K^+K^- and $K_s^0K_s^0$. Figure 17 displays an example for each of those two modes obtained by DM2 [76] and Mark III [103]. The main features are two well separated peaks due to f'(1525) and Θ(1700).

Due to lower final state multiplicities, the channel with the higher statistics is K^+K^-. This channel has provided the most precise information on branching ratios, mass and width values, and polarization parameters. Averaging all mass and width determinations yields [103, 76]

$$M_{f'} = (1530 \pm 8)\ \text{MeV}, \qquad \Gamma_{f'} = (95 \pm 23)\ \text{MeV}, \tag{6.4}$$

where statistical and systematic errors have been added in quadrature. These values agree well with those stated in the Review of Particle properties [59]: $M_f = (1525 \pm 5)$ MeV and $\Gamma_{f'} = (70 \pm 10)$ MeV.

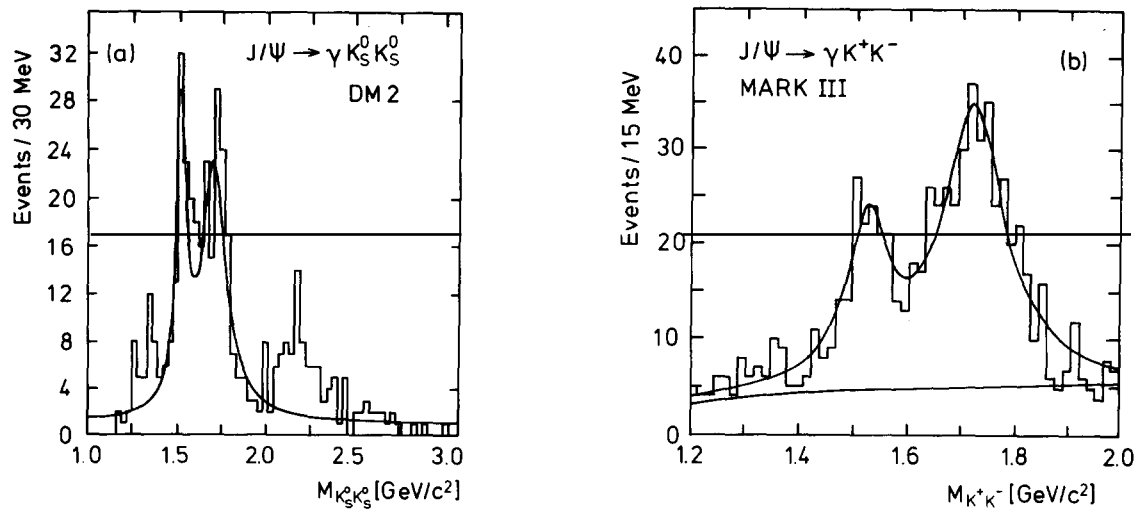

Fig. 17. Invariant $K\bar{K}$ mass distributions from (a) DM2 $J/\psi \to \gamma K_s^0 K_s^0$ and (b) Mark III $J/\psi \to \gamma K^+ K^-$. The solid curves represent a fit with two Breit-Wigner line shapes and three-body phase space. In (a) the f′ mass and widths are fixed at their nominal values. In both cases the two Breit-Wigners are added incoherently.

Mark III has tried several parametrizations to the whole structure, taking into account interference between the two signals. A fit with minimum interference [103] in the dip between the two peaks gives a good description. But this fit is nearly indistinguishable from a purely incoherent fit. One concludes that there is no significant evidence for interference effects and Mark III takes the number of events attributed to each resonance from the incoherent fit. DM2 allows in the K^+K^- channel for interference with the relative phase fixed at π. Listed in table 13 are the obtained product branching ratios. Iso-spin factors have been taken into account and K^+K^- and $K^0\bar{K}^0$ have been averaged, where appropriate. Summing all known branching ratios yields

$$BR(J/\psi \to \gamma f'(1525)) = (6.0 \pm 1.1) \times 10^{-4}\,, \tag{6.5}$$

assuming no other substantial decay modes to exist for the f′.

Taking the ratio of the radiative branching fractions to f′ and f (eqs. (6.5) and (6.1)) gives

Table 13
Summary of product branching ratio measurements on f′(1525) and Θ(1700) in units of 10^{-4}, K^+K^- and $K^0\bar{K}^0$ have been averaged when two measurements were available. Statistical and systematic erors have been added in quadrature.

Branching ratio × 10^4	Ref.	Mark II 147	Crystal Ball 60	Mark III 103	DM2 76
$J/\psi \to \gamma f'$	$f' \to K\bar{K}$	1.8 ± 1.2		4.9 ± 1.3	3.5 ± 0.7
	$f' \to \eta\eta$		1.9 ± 0.9		
	$f' \to \pi\pi$				~0.7
$J/\psi \to \gamma\Theta$	$\Theta \to K\bar{K}$	12.0 ± 5.4		9.4 ± 1.8	7.5 ± 1.3
	$\Theta \to \eta\eta$		2.6 ± 1.1		
	$\Theta \to \pi\pi$	< 3.2	2.3 ± 1.1	2.4 ± 0.8	1.8 ± 0.4

$R_{f'/f} = 0.4 \pm 0.1$. In the standard radiative J/ψ decay diagram, the photon is radiated from the initial state and the two-gluon system is an SU(3) flavor singlet. Thus it projects out the singlet part of the f, f' wave functions, which happen to be ideally mixed. The naive SU(3) prediction is therefore $R_{f'/f} = \tan^2 35° \simeq 0.5$. Taking into account phase space and α_s corrections [93] changes the prediction to $R_{f'/f} \sim 0.3$, consistent with the data.

6.3. $J/\psi \to \gamma + \Theta(1700)$

The Θ(1700) was discovered by the Crystal Ball [155] group in the channel $J/\psi \to \gamma\eta\eta$ and its spin-parity was measured to be 2^+. To take into account the possibility of an additional f' signal, they have reanalyzed their data [60] (fig. 18) and have fit the spectrum to two non-interfering Breit–Wigner functions, with the masses and widths of f' and Θ fixed at the Mark III values. They obtained the branching ratios listed in table 13. Note that the G(1590), found by GAMS [156] in the final state ηη, has spin-parity 0^+ and is thus different from Θ and f'.

Mark II, Mark III and DM2 have analyzed the Θ(1700) in the final state K^+K^- (see section 6.2. on f'(1525)). In addition, Mark III and DM2 have found a signal in $K_s^0K_s^0$. The ratio of product branching ratios to those two final states is 2.8 ± 0.8, consistent with a value of 2 expected if the Θ has isospin zero. With this assignment the different measurements of the product branching ratios can be combined. The averages are listed in table 13. Included are the determinations of the rate $J/\psi \to \Theta$, $\Theta \to \pi\pi$ discussed in section 6.1. Summing all known branching ratios and taking their relative ratios yields

$$\mathrm{BR}(J/\psi \to \gamma\Theta) = (1.3 \pm 0.2) \times 10^{-3}, \qquad K\bar{K} : \eta\eta : \pi\pi \simeq 3 : 1 : 0.8 . \tag{6.6}$$

Other decay modes were searched for, but none could be found. Upper limits were calculated for the

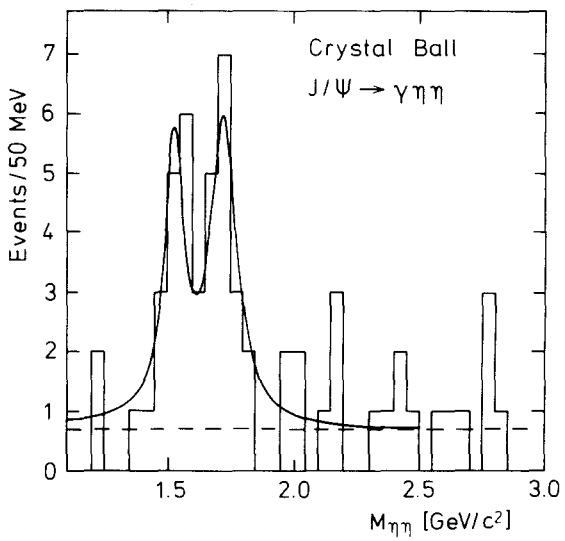

Fig. 18. Crystal Ball invariant ηη mass distributions from $J/\omega \to \gamma\eta\eta$. The spectrum is fit to two non-interfering Breit–Wigner line shapes plus a flat background.

decay modes: $\eta\eta'$ [135], $\rho\rho$[142], $\omega\omega$[143] and $K\bar{K}\pi$, $K^+K^-\pi^+\pi^-$ [103] with values of {2.1, 5.5, 2.4 and 2.8, 1.0} $\times 10^{-4}$, respectively. The average mass and width from all experiments is

$$M_\Theta = (1710 \pm 5)\,\text{MeV}\,, \qquad \Gamma_\Theta = (153 \pm 10)\,\text{MeV}\,,$$

where statistical and systematic errors have been added in quadrature.

Maximum likelihood analyses of the decay angular distributions have been performed by all four experiments. DM2 and Mark III reject spin zero for the f′ with very high probability. For the Θ, Mark III has found 2^+ to be favored over 0^+ at a confidence level of $\sim 99.9\%$, confirming the Crystal Ball spin assignment. The Mark II and DM2 experimental data are also consistent with 2^+. In addition, DM2 and Mark III have measured the helicity amplitude ratios x and y. The surprising results are stated in table 12. In contrast to the small helicity 2 amplitude y measured for the f and f′, the Θ(1700) is produced with approximately equal strength in all three helicity states. This is indicative of a different nature of the Θ(1700). The Crystal Ball and Mark II polarization parameters x differ in sign from those determined by Mark III and DM2. It turns out that all helicity analyses yield two likelihood maxima symmetric with respect to $x = 0$. With low statistics event samples it is difficult to determine the sign of x unambiguously.

Many review articles analyze the possible nature of the Θ(1700), see for instance refs. [98, 121, 157]. In the following, the different possibilities will be evaluated in order of increasing plausibility. Of central importance is the decay pattern of the Θ stated in eq. (6.6). If the Θ(1700) were a normal $q\bar{q}$ state, the preferred decay to $K\bar{K}$ would point to an $s\bar{s}$ content. This cannot be, however, as the f′ is definitely the $s\bar{s}$ state in the tensor nonet, and quark models do not allow excitations of the f′ to be so close in mass. For instance, the orbital excitation of the f is the h(2030) and the radially excited f′ is expected [127] at about 2050 MeV. Also the different helicity structure with respect to f and f′ point in the direction of a non-$q\bar{q}$ content in the Θ.

A second possibility would be a hybrid meson. Their spectra and decay pattern have been investigated by many authors [9, 158]. The general result for a 2^{++} state is in the rather high mass range of 1.9–2.3 GeV. A favorite decay of hybrids is to two vector mesons containing strange quarks such as K*K* and the decay to two pseudoscalars is strongly suppressed. Given these results it seems unlikely that the Θ is a hybrid meson.

The possibility of a $q\bar{q}q\bar{q}$ state may be more likely. Normally these states are expected [113] to be very broad, except maybe for the 0^{++}. However, the $(u\bar{u} + d\bar{d})s\bar{s}$ state would have a mass below the threshold for a normal 'fall apart' mode, and could thus be substantially narrower. In this case one would expect: $\Gamma(\Theta \to K\bar{K}) \simeq \Gamma(\Theta \to \eta\eta)$, not totally inconsistent with experiment. Given the rather large production rate of the Θ, we would expect to see other potential four-quark states. But even the strongest candidate for a $q\bar{q}q\bar{q}$ meson, the S*(975), has failed to show up in radiative ψ decays.

The last possibility is a gluonium hypothesis. Certainly mass and width predictions qualify the Θ(1700) as a gluonic meson [85, 90, 88]. But it is the decay pattern, which causes problems. A gluonic meson is by nature a flavor singlet, and so the decay rates should be related by SU(3) to

$$K\bar{K} : \eta\eta : \pi\pi \simeq 3 : 0.5 : 6\,,$$

when D-wave phase space corrections are taken into account. Obviously the Θ does not follow this rule. It has been argued though, that in the bag model many gluonic mesons prefer to decay into strange quarks [159]. In addition, mixing of the Θ with the nearby f′ (or excitations thereof) [160] might alter the decay pattern appreciably. Recently, the CERN OMEGA group WA76 [161] found a signal in the K^+K^-

system produced centrally in $\pi^+ p \to \pi^+ (K^+ K^-) p$ and pp scattering. One of the structures seen is compatible with the Θ(1700) in mass and width. The observation of the Θ in such double-pomeron exchange reactions is indicative of its gluon content. Summarizing, there are very strong indications that the Θ(1700) is really something new. What its nature is remains to be answered, but a gluonic or four-quark state is the most likely explanation.

7. Other decays

In the first section the unusual properties of the ξ(2200) are reviewed. Its high mass together with a width consistent with zero make this state a very interesting resonance. The second section covers the search for the axion, a particle predicted in theories of the strong interactions. In the third section radiative decays from J/ψ and ψ′ are compared. An unusual pattern emerges.

7.1. $J/\psi \to \gamma + \xi(2200)$

In 1983 the Mark III group presented evidence [103, 162] for a heavy narrow resonance, the ξ(2200), decaying to K^+K^-. The statistical significance was about 4.6σ, with additional evidence in the $K_s^0 K_s^0$ channel. Both signals were based on 2.7 million J/ψ decays and depended heavily on the precise timing information from the Mark III time-of-flight system in order to discriminate pions from kaons. A spin-parity analysis had been tried, but could not distinguish between spin 0, 2, or 4.

One problem existed for this first observation of the ξ. Two data sets were accumulated a year apart and did not quite agree with each other. A ξ mass shift of 40 MeV could only be explained by a change of detector performance. It was the larger data set taken later in time that provided the more significant signal. The DM2 collaboration [76] has analyzed 8.7 million J/ψ decays. They required only one kaon to be compatible with TOF information. The absence of a signal for the ξ(2200) is translated into an upper limit of $BR(J/\psi \to \gamma\xi, \xi \to K^+K^-) < 1.2 \times 10^{-5}$ at the 95% confidence level, assuming a narrow ξ. They also analyzed the $K_s^0 K_s^0$ channel (see fig. 17a). The peak evident in the 2.2 GeV region is by one bin too low to be associated with the ξ. Using this bin anyway, they have calculated an upper limit of $BR(J/\psi \to \gamma\xi, \xi \to K^0\bar{K}^0) < 2.0 \times 10^{-5}$.

In 1985, Mark III accumulated another sample of 3.1 million J/ψ data. The ξ repeated in this data set [163]. Summing all their data, Mark III has obtained the following parameters:

$$BR(J/\psi \to \gamma\xi) \times BR(\xi \to K^+K^-) = (4.2^{+1.9}_{-1.6}) \times 10^5 ,$$

$$BR(J/\psi \to \gamma\xi) \times BR(\xi \to K_s^0 K_s^0) = (3.2^{+1.8}_{-1.5}) \times 10^{-5} ,$$

$$M_\xi = (2231 \pm 8)\ \text{MeV} , \qquad \Gamma_\xi = (22^{+18}_{-14})\ \text{MeV} ,$$

where statistical and systematic errors have been averaged. A statistical significance of 4.5σ and 3.6σ was stated for the two channels, respectively, see fig. 19. The ratio of branching fractions for the decay modes K^+K^- and $K_s^0 K_s^0$ of 1.3 ± 0.9 is consistent with a value 2 expected for an isoscalar meson. Other decay modes have been searched for but none could be found. Of particular interest concerning theoretical models are the decays to $\mu^+\mu^-$ and ππ. The corresponding upper limits on the product branching ratios are 5×10^{-6} and 2×10^{-5}, respectively.

Possible explanations for such a narow, high mass state include a normal $q\bar{q}$ meson, a gluonic and

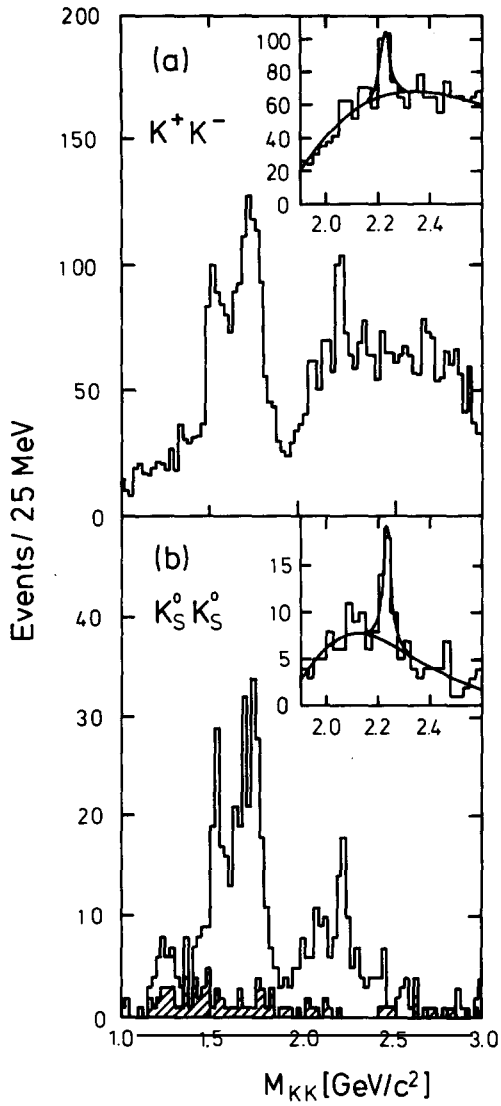

Fig. 19. Mark III invariant $K\bar{K}$ mass distributions from (a) $J/\psi \to \gamma K^+K^-$ and (b) $J/\psi \to \gamma K^0_S K^0_S$ with four-pion background cross-hatched. Fits to the region around the $\xi(2200)$ are shown in the insets.

hybrid meson, and a Higgs boson. A short evaluation follows for each of these hypotheses. If the ξ is made of quarks alone, the observed $K\bar{K}$ decay requires them to be strange quarks. Godfrey et al. have pointed out [164], that a candidate may be the $L = 3$ $s\bar{s}$ meson, an orbital excitation of the $f'(1525)$. Due to a limited number of decay modes available, the total width is only 50 MeV, compatible with experiment. Also the product branching ratio compares favorably with the data. The picture of an excited $s\bar{s}$ meson fits the ξ rather well and makes this the overall preferred theoretical explanation.

For a gluonium interpretation, the ξ mass seems too high. However, Ward has shown [165], that the ξ fits a 0^{++} gluonic meson interpretation in the context of the bag model. Here the decay to $\pi^+\pi^-$ is expected to be strongly suppressed. Another sugestion concerns a hybrid meson. Only a 2^{++} hybrid

meson would be narrow enough [158] to make the ξ qualify, but the predicted production rate is too small in comparison with experiment.

Finally, the ξ has been suggested [166, 167] to be the long sought after Higgs boson of the electroweak theory. Its coupling to fermions is proportional to the fermion mass. A 2 GeV Higgs would thus favor $s\bar{s}$ final states. The radiative decay rate from J/ψ has been calculated [168]:

$$\mathrm{BR}(J/\psi \to \gamma H^0) = (3.1 \pm 0.5) \times 10^{-5}\,, \tag{7.1}$$

but is too small to account for the experimental rate. In addition, the mass of the neutral Higgs is bound to be larger than 7 GeV [169]. A way out of these discrepancies is to introduce two Higgs doublets in the electroweak theory [170], changing the prediction (7.1) by the square of the ratio of the two vacuum expectation values of the Higgs fields. But results on radiative transitions from the Υ(1S) and B meson decays [171] together with the Mark III limits on $\xi \to \pi\pi$ and $\xi \to \mu\mu$ seem to rule out this scenario. Summarizing, it appears that the standard hypothesis of an orbitally excited $s\bar{s}$ state is the most appealing. Nothing new has to be introduced and predictions are quite consistent with experimental data.

7.2. *J/ψ → γ + axion*

The axion is a Goldstone boson which appears after the breaking [172] of a U(1) symmetry. This symmetry is imposed [173] on the Lagrangian to circumvent large *P* and *CP* violations of the strong interactions. The standard axion has a small mass $m_a \simeq \mathcal{O}(100\ \mathrm{keV})$ and a long lifetime $\tau_a \simeq \mathcal{O}(10^{-2\pm2}\mathrm{s})$. Early experimental results on axion production and/or decay were controversial, either observing [174] the decay of an axion-like particle of mass $m_a \simeq 250$ keV, or ruling out [175] the existence of a standard axion.

The predicted radiative decay rate for a vector meson into an axion contains a free parameter x, the ratio of the vacuum expectation values of the two Higgs fields in the theory. The rate also depends on whether the heavy quarks in the meson are up-like (charge 2/3) or down-like (charge −1/3). For the up-like J/ψ the prediction is [176]

$$\frac{\mathrm{BR}(J/\psi \to \gamma a)}{\mathrm{BR}(J/\psi \to \mu^+\mu^-)} = \frac{G_F m_c^2}{\sqrt{2}\pi\alpha_{em}}\, x^2\,, \tag{7.2}$$

where G_F is the Fermi coupling constant and m_c is the current mass of the charmed quark. The corresponding prediction for the Υ(1S) is obtained by replacing x^2 by $1/x^2$ in eq. (7.2). With $m_c = (1.5 \pm 0.3)$ GeV and the experimentally determined leptonic branching ratio [59] we get the prediction $\mathrm{BR}(J/\psi \to \gamma a) = (5.7 \pm 1.4) \times 10^{-5} x^2$.

The Crystal Ball [177] searched for the axion in radiative J/ψ events. As the axion will not decay in the detector, the signature is one photon of beam energy and nothing else. No signal was observed which gave an upper limit on the branching ratio of

$$\mathrm{BR}(J/\psi \to \gamma a) < 1.4 \times 10^{-5}$$

at the 90% confidence level. The corresponding upper limit on $x < 0.6$ ruled out a value of $x = 3.0 \pm 0.3$ found earlier [174].

To eliminate any x dependence when comparing with theoretical predictions, a test had been proposed

[178] to combine the predictions on J/ψ and Υ(1S) radiative decays. In the product of both branching ratios the unknown parameter x cancels and one obtains the prediction $BR(J/\psi \to \gamma a) \times BR(\Upsilon \to \gamma a) = (1.6 \pm 0.3) \times 10^{-8}$. The Crystal Ball upper limit together with the limit on the corresponding branching ratio from CESR [179] yields a product of less than 0.4×10^{-8} which is clearly below the prediction. Therefore the standard axion has been ruled out completely by experiment. After this negative result, invisible axions [180] have attracted more theoretical interest. Unfortunately, they are by nature of little experimental interest.

7.3. Comparison of J/ψ and ψ′ radiative decays

In the introduction to chapter 4 it was shown that the partial widths of the J/ψ to three gluons and to a photon plus two gluons are proportional to the square of the wave function at the origin (see eqs. (4.1) and (4.2)), as is the partial width to leptons. Assuming that the hadronization of gluons is not substantially different at the mass of the ψ′ than at the mass of the J/ψ, one obtains the ratios [181]

$$BR(\psi' \to \gamma X)/BR(J/\psi \to \gamma X) = BR(\psi' \to Y)/BR(J/\psi \to Y) = BR(\psi' \to \mu^+\mu^-)/BR(J/\psi \to \mu^+\mu^-) ,$$

where X and Y are any arbitrary non-charmonium states. Using the measured leptonic branching ratios [59] of the J/ψ and ψ′ yields the prediction

$$BR(\psi' \to \gamma X)/BR(J/\psi \to \gamma X) = (12 \pm 2)\% , \tag{7.3}$$

ignoring phase-space effects.

This ratio was determined by Mark II [181] for several hadronic final states such as $p\bar{p}$, $p\bar{p}\pi^+\pi^-$, $K^+K^-\pi^+\pi^-$, $p\bar{p}\pi^0$, $2\pi^+2\pi^-\pi^0$ and $3\pi^+3\pi^-\pi^0$. For all of them the ratio of branching fractions was found to be in good agreement with the theoretical prediction (7.3). However, two final states, ρπ and K*K, are unobserved on the ψ′ at levels five and sixteen below the predicted rate at the 90% confidence level.

The Crystal Ball collaboration has studied this ratio for radiative decays [60] and obtained

$$\begin{aligned} &BR(\psi' \to \gamma f)/BR(J/\psi \to \gamma f) = (9 \pm 3)\% , \quad BR(\psi' \to \gamma\Theta)/BR(J/\psi \to \gamma\Theta) < (10\text{–}15)\% , \\ &BR(\psi' \to \gamma\eta)/BR(J/\psi \to \gamma\eta) < 1.8\% , \quad BR(\psi' \to \gamma\eta')/BR(J/\psi \to \gamma\eta') < 2.6\% . \end{aligned} \tag{7.4}$$

Upper limits are at the 90% confidence level. The upper limit for the radiative decay to the Θ is uncertain due to the possible presence of an f′ signal in the J/ψ data.

It is apparent that four decays (ρπ, K*K, γη and γη′) are suppressed on the ψ′ compared to the lowest order QCD prediction relative to the corresponding J/ψ decays. It is interesting to note that all four final states consist of a vector and a pseudoscalar particle. Karl and Roberts [182] have suggested that there is an oscillation in the amplitude for three gluons to hadronize to the ρπ and K*K final states which has a node at the mass of the ψ′. It is not clear whether this explanation can also account for the observed suppression of the γη and γη′ final states. Hou and Soni [183] have postulated the existence of a vector gluonic meson near 2.4 GeV which mixes with the J/ψ to enhance the decays $J/\psi \to \rho\pi$ and $J/\psi \to K^*K$ but is too far in mass from the ψ′ to enhance its decays. Again, it is not obvious that such a gluonic meson would couple substantially to the final states γη and γη′. Summarizing, it seems that the violation of the

'12% rule' is not understood at present. Its solution will provide new clues to a better understanding of quarkonia decay mechanisms. One decay mode that might help disentangle this problem is the decay to vector plus tensor particles.

8. Conclusions

Radiative decays in the ψ family have proven to yield an abundance of information on states within the charmonium system and low mass $q\bar{q}$ states. It has been shown that most of the experimental data on the χ and the η_c states are in good agreement with theoretical predictions. An early problem concerning the radiative width of $\psi' \to \gamma\chi$ has been solved by inclusion of relativistic corrections and coupled channel effects. A factor of 2 problem still exists between theory and the measured values for the magnetic dipole transition rate $J/\psi \to \gamma\eta_c$ and the total hadronic width of the χ_0. Further experiments should help to clarify this deviation. Overall, an impressive qualitative agreement emerges between charmonium spectroscopy and theoretical models. The successful application of such diverse approaches as QCD sum-rules and potential models have guided us from the first observation of the J/ψ to a detailed understanding of the inter-quark force.

In contrast to the well-understood charmonium states, many puzzles remain in the light meson sector. Radiative transitions to pseudosclalar and tensor mesons have helped to understand the mixing pattern within nonets. In particular, it was found that the η′ needs some additional component in its wave function to understand the large production rate in radiative J/ψ decays. The most likely admixture is in the form of gluons. But where is the gluonic state to mix with the η′? The new state ι(1460) is certainly a

Table 14
Summary of radiative decays in the ψ family to exclusive final states. Branching ratios are determined by summing over all known decay modes.

$J/\psi \to \gamma X$ X =	BR($J/\psi \to \gamma X$) (in units of 10^{-3})	Decay modes	$J^P(X)$
π^0	0.038 ± 0.008	$\gamma\gamma$	0^-
η	0.88 ± 0.06	$\gamma\gamma$, $\gamma\pi^+\pi^-$, $3\pi^0$	0^-
η′	3.9 ± 0.3	$\eta\pi\pi$, $\gamma\rho^0$, $\gamma\omega$, $\gamma\gamma$	0^-
f(1270)	1.35 ± 0.11	$\pi^+\pi^-$, $\pi^0\pi^0$	2^+
ι(1460)	6.3 ± 0.5	$K\bar{K}\pi$, $\gamma\rho^0$, ρρ, ωω	0
f′(1525)	0.60 ± 0.11	K^+K^-, $K_s^0K_s^0$, ππ?, ηη?	2^+
Θ(1700)	1.3 ± 0.2	$K\bar{K}$, ηη, ππ	2^+
X(1770)	6.1 ± 1.0	ηππ	
X(1800)	1.0 ± 0.2	ρρ	0^-
X(2065)	0.35 ± 0.06	$\pi^+\pi^-$, $\pi^0\pi^0$	$(\text{even})^+$
ξ(2235)	0.10 ± 0.03	K^+K^-, $K_s^0K_s^0$	$(\text{even})^+$
$\eta_c(2980)$	12.7 ± 3.6	$\eta\pi\pi$, $K\bar{K}\pi$, $\eta'\pi\pi$, etc.	0^-
$\psi' \to \gamma X$ X =	BR($\psi' \to \gamma X$) (in units of 10^{-3})	Decay modes	$J^P(X)$
$\eta_c(2980)$	2.8 ± 0.6	$K\bar{K}\pi$, $2(\pi\pi)$, $\pi\pi K\bar{K}$	0^-
$\chi_0(3415)$	94 ± 8	$\gamma J/\psi$, $2(\pi\pi)$, $\pi^+\pi^-$, etc.	0^+
$\chi_1(3511)$	86 ± 8	$\gamma J/\psi$, $2(\pi\pi)$, etc.	1^+
$\chi_2(3557)$	78 ± 8	$\gamma J/\psi$, $2(\pi\pi)$, $\pi^+\pi^-$, etc.	2^+
$\eta_c'(3594)$	2–13		

good candidate. Both, ι(1460) and Θ(1700) seem to have a large gluon content. An evaluation of production and decay properties shows the Θ to be a strong gluonium candidate. The ι is more controversial. A detailed understanding of the excited pseudoscalar nonet is necessary before the ι can be classified. Future information on J/ψ hadronic decays to ι and Θ should help settle this question. A final answer is very important, as the existence of gluonic mesons constitutes strong evidence for the non-Abelian nature of QCD. Considerable excitement was caused by the observation of a particle ξ(2200) found in 1983. New evidence by the same experiment confirms the signal, but it is not seen in another large statistics experiment. The question on its existence is thus still open. A likely explanation would be an orbital excitation of the tensor meson f'(1525).

Table 14 summarizes the presently known radiative branching ratios from the J/ψ and the ψ'. Excluding the η_c, radiative decays from J/ψ to exclusive final states sum to a branching ratio of about 2%, only ~1/4 of the theoretical prediction. But an analysis of the inclusive photon spectrum has shown the total rate to be consistent with expectation. The shape of the spectrum, however, differs from QCD predictions. Incorporation of non-perturbative effects will change the shape, but will have little influence on the rate. Given the missing radiative branching fraction to exclusive final states, it seems that J/ψ radiative decays will continue to surprise us.

Acknowledgements

I am indepted to my colleagues in the Crystal Ball and Mark III collaborations for many interesting and fruitful discussions on the material presented here. Particular thanks go to Elliott Bloom, Susan Cooper, Achim Irion, Helmut Marsiske and Peter Schmitt for corrections and clarifications that resulted from their careful reading of the manuscript. It is a pleasure to acknowledge stimulating conversations with Manfred Böhm and Max Scheer. Finally, I would like to acknowledge the hospitality received at DESY and SLAC.

References

[1] M. Gell-Mann, Phys. Lett. 8 (1964) 214;
G. Zweig, CERN TH-412.
[2] J.J. Aubert et al.,, Phys. Rev. Lett. 33 (1974) 1404.
[3] J.E. Augustin et al., Phys. Rev. Lett. 33 (1974) 1406.
[4] G. Goldhaber et al., Phys. Rev. Lett. 37 (1976) 255.
[5] S.W. Herb et al., Phys. Rev. Lett. 39 (1977) 252.
[6] S.L. Glashow, Nuc. Phys. 22 (1961) 579;
S. Weinberg, Phys. Rev. Lett. 19 (1967) 1264;
A. Salam, in: Elementary Particle Theory, ed. N. Swartholm (Almquist and Wiksell, Stockholm, 1968) p. 367.
[7] H. Fritsch and M. Gell-Mann, Proc. XVI Int. Conf. on High Energy Physics, Vol. 2 (Chicago, 1972) p. 135;
H. Fritsch, M. Gell-Mann and H. Leutwyler, Phys. Lett. 47B (1973) 365;
H.D. Politzer, Phys. Rev. Lett. 30 (1973) 1346;
D.J. Gross and F. Wilczek Phys. Rev. D 8 (1973) 3633;
S. Weinberg, Phys. Rev. Lett. 31 (1973) 494.
[8] H. Fritsch and P. Minkowski, Nuovo Cim. 30A (1975) 393;
P.G.O. Freund and Y. Nambu, Phys. Rev. Lett. 34 (1975) 1645;
R.L. Jaffe and K. Johnson, Phys. Lett. 60B (1976) 201;
T. Barnes, Zeit. Phys. C 10 (1981) 275;
C.E. Carlson, J.J. Coyne, P.M. Fishbane, F. Gross and S. Meshkov, Phys. Lett. 99B (1981) 353.

[9] P. Hasenfratz, R.R. Horgan, J. Kuti and J.M. Richard, Phys. Lett. 95B (1980) 299;
M. Chanowitz and S. Sharpe, Nucl. Phys. B 222 (1983) 211;
T. Barnes, F.E. Close and F. de Viron, Nucl. Phys. B 224 (1983) 241.
[10] E.D. Bloom and C.W. Peck, Ann. Rev. Nucl. Part. Sci. 33 (1983) 143;
M. Oreglia et al., Phys. Rev. D 25 (1982) 2259.
[11] J.E. Augustin et al., Physica Scripta 23 (1981) 623.
[12] G.S. Abrams et al., Phys. Rev. Lett. 43 (1979) 477, 481;
W. Davies-White et al., Nucl. Instr. Methods 160 (1979) 227.
[13] D. Bernstein et al., Nucl. Instr. Methods 226 (1984) 301;
J. Roehrig et al., Nucl. Instr. Methods 226 (1984) 319.
[14] R. Brandelik et al., Zeit. Phys. C 1 (1979) 233.
[15] W. Bartel et al., Phys. Lett. 64B (1976) 483.
[16] J. Burmester et al., Phys. Lett. 66B (1977) 395.
[17] G. Gidal, B. Armstrong and A. Rittenberg, Particle Data Group, Berkeley, LBL-91.
[18] J.E. Augustin et al., Phys. Rev. Lett. 34 (1975) 233.
[19] C.J. Biddick et al., Phys. Rev. Lett. 38 (1977) 1324.
[20] S.L. Glashow, J. Iliopoulos and L. Maiani, Phys. Rev. D 2 (1970) 1285.
[21] T. Appelquist and H.D. Politzer, Phys. Rev. Lett. 34 (1975) 43.
[22] A. DeRújula and S.L. Glashow, Phys. Rev. Lett. 34 (1975) 46.
[23] G.S. Abrams et al., Phys. Rev. Lett. 33 (1974) 1453.
[24] T. Appelquist, A. DeRújula, H.D. Politzer and S.L. Glashow, Phys. Rev. Lett. 34 (1975) 365.
[25] W. Braunschweig et al., Phys. Lett. 57B (1975) 407.
[26] G.J. Feldman et al., Phys. Rev. Lett. 35 (1975) 821.
[27] W. Braunschweig et al., Phys. Lett. 67B (1977) 243.
[28] J.S. Whitaker et al., Phys. Rev. Lett. 37 (1976) 1596.
[29] W. Bartel et al., Phys. Lett. 79B (1978) 492.
[30] S.W. Otto and J.D. Stack, Phys. Rev. Lett. 52 (1984) 2328.
[31] C. Quigg and J.L. Rosner, Phys. Rep. 56 (1979) 167.
[32] A. Martin, Phys. Lett. 93B (1980) 338 and Phys. Lett. 100B (1981) 511;
A. Khare, Phys. Lett. 98B (1981) 385.
[33] E. Eichten, K. Gottfried, T. Kinoshita, K.D. Lane and T.M. Yan, Phys. Rev. D17 (1978) 3090 and Phys. Rev. D21 (1980) 203;
T. Appelquist, R.M. Barnett and K. Lane, Ann. Rev. Nucl. Part. Sci. 28 (1978) 387.
[34] A.B. Henriques, B.H. Kellet, R.G. Moorhouse, Phys. Lett. 64B (1976) 85.
[35] G. Bhanot and S. Rudaz, Phys. Lett. 78B (1978) 119.
[36] H. Krasemann and S. Ono, Nucl. Phys. B 154 (1978) 283.
[37] J.L. Richardson, Phys. Lett. 82B (1979) 272.
[38] W. Buchmüller, G. Grunberg and S.H.H. Tye, Phys. Rev. Lett. 45 (1980) 103, and erratum Phys. Rev. Lett. 45 (1980) 587;
W. Buchmüller and S.H.H. Tye, Phys. Rev. D 24 (1981) 132.
[39] D.W. Duke and R.G. Roberts, Phys. Rep. 120 (1985) 275.
[40] J.S. Kang and H.J. Schnitzer, Phys. Rev. D 12 (1975) 842.
[41] E. Eichten and F. Feinberg, Phys. Rev. Lett. 43 (1979) 1205 and Phys. Rev. D 23 (1981) 2724.
[42] D. Gromes, Nucl. Phys. B 131 (1977) 80.
[43] J. Pumplin, W. Repko, A. Sato, Phys. Rev. Lett. 35 (1975) 1538;
H. Schnitzer, Phys. Rev. Lett. 35 (1975) 1540.
[44] D. Gromes, Zeit. Phys. C 26 (1984) 401.
[45] W. Buchmüller, Phys. Lett. 112B (1982) 479 and Proceedings of the Moriond Workshop on New Flavors, Les Arcs, France, January 1982.
[46] H.A. Bethe and E.E. Salpeter, Quantum Mechanics of One and Two Electron Atoms (Springer Verlag, Berlin, 1957);
M.G. Olsson, Phys. Rev. D 28 (1983) 1223.
[47] V.A. Novikov et al., Phys. Rep. 41 (1978) 1.
[48] R. McClary and N. Byers, Phys. Rev. D 28 (1983) 1692.
[49] V. Zambetakis and N. Byers, Phys. Rev. D 28 (1983) 2908.
[50] T. Appelquist and H.D. Politzer, Phys. Rev. D 12 (1975) 1404 and Phys. Rev. Lett. 34 (1975) 43.
[51] R. Barbieri, R. Gatto and R. Kögerler, Phys. Lett. 60B (1976) 183;
R. Barbieri, R. Gatto and E. Remiddi, Phys. Lett. 61B (1976) 465.
[52] L.D. Landau, Sov. Phys. Doklady 60 (1948) 207;
C.N. Yang, Phys. Rev. 77 (1950) 242.
[53] R. Barbieri, M. Caffo, R. Gatto and E. Remiddi, Phys. Lett. 95B (1980) 93;
R. Barbieri, R. Gatto and E. Remiddi, Phys. Lett. 106B (1981) 497.

[54] W. Tannenbaum et al., Phys. Rev. D 17 (1978) 1731.
[55] J.E. Gaiser et al., SLAC-PUB 2899, submitted to Phys. Rev. D.
[56] W. Bartel et al., Phys. Lett. 79B (1978) 492.
[57] T.M. Himel et al., Phys. Rev. Lett. 44 (1980) 920.
[58] M. Oreglia et al., Phys. Rev. D 25 (1982) 2259 and PhD thesis, SLAC-236 (1980).
[59] Particle Data Group: Review of Particle Properties, Rev. Mod. Phys. 56, II (1984).
[60] R.A. Lee, PhD Thesis, SLAC-282 (1985).
[61] C. Baglin, Proc. Int. Conf. Physics in Collision, Autun, France, 1985.
[62] J. Baacke, Y. Igarashi and G. Kasperidus, Zeit. Phys. C 13 (1982) 131.
[63] P. Falkensteiner, D. Flamm and F. Schöberl, Zeit. Phys. C 23 (1984) 275.
[64] H. Grotch, D.A. Owen and K.L. Sebastian, Phys. Rev. D 30 (1984) 1924.
[65] M.G. Olsson, A.D. Martin and A.W. Peacock, Phys. Rev. D 31 (1985) 81.
[66] The data on the $b\bar{b}$ χ states are from those experiments which observe all three states unambiguously.
ARGUS collab.: H. Albrecht et al., Phys. Lett. 160B (1985) 331;
Crystal Ball collab.: R. Nernst et al., Phys. Rev. Lett. 54 (1985) 2195, and W.Walk et al., SLAC-PUB-3575 and DESY 85-019, submitted to Phys. Rev. D.
[67] S.N. Gupta, S.F. Radford and W.W. Repko, Phys. Rev. D 26 (1982) 3305 and Phys. Rev. D 30 (1984) 2424.
[68] L.J. Reinders, H.R. Rubinstein and S. Yazaki, Phys. Rep. 127 (1985) 1.
[69] K. Königsmann, Proc. 5th Int. Conf. Physics in Collision, Autun, France, 1985, and DESY 85-089 (1985).
[70] K. Hagiwara, S. Jacobs, M.G. Olsson and K.G. Miller, Phys. Lett. 131B (1983) 455.
[71] R. Partridge et al., Phys. Rev. Lett. 44 (1980) 712.
[72] R. Partridge et al., Phys. Rev. Lett. 45 (1980) 1150.
[73] T.M. Himel et al., Phys. Rev. Lett. 45 (1980) 1146.
[74] R. Partridge et al., Phys. Rev. Lett. 48 (1982) 70.
[75] R.M. Baltrusaitis et al., Phys. Rev. Lett. 52 (1984) 2126.
[76] J.E. Augustin et al., LAL/85-27 (1985).
[77] R.M. Baltrusaitis et al., Phys. Rev. D 33 (1986) 629.
[78] C. Quigg and J.L. Rosner, Phys. Rev. D 16 (1977) 1497.
[79] H.E. Haber and J. Perrier, Phys. Rev. D 32 (1985) 2961.
[80] M.A. Shifman, Zeit. Phys. C 4 (1980) 345;
M.A. Shifman and M.I. Vysotsky, Zeit. Phys. C 10 (1981) 131;
T.M. Aliyev, Zeit. Phys. C 26 (1984) 275;
V.A. Beilin and A.V. Radyushkin, Nucl. Phys. B 260 (1985) 61.
[81] K. Königsmann, Proceedings of the 17th Rencontre de Moriond; Les Arcs, France, 1982; and SLAC-PUB-2910.
[82] Ch. Berger et al., Phys. Lett. 167B (1986) 120.
[83] P.B. Mackenzie and G.P. Lepage, Phys. Rev. Lett. 47 (1981) 1244;
S.J. Brodsky, G.P. Lepage and P.B. Mackenzie, Phys. Rev. D 28 (1983) 228.
[84] M.T. Ronan et al., Phys. Rev. Lett. 44 (1980) 367.
[85] M. Chanowitz and S. Sharpe, Nucl. Phys. B 222 (1983) 211.
[86] D.L. Scharre et al., Phys. Rev. D 23 (1981) 43;
G.S. Abrams et al., Phys. Rev. Lett. 44 (1980) 114.
[87] S.J. Brodsky et al., Phys. Lett. 73B (1978) 203.
[88] C.E. Carlson, T.H. Hansson and C. Peterson, Phys. Rev. D 30 (1984) 1594.
[89] B. Berg and A. Billoire, Nucl. Phys. B 221 (1983) 109 and Nucl. Phys. B 226 (1983) 405.
[90] K. Ishikawa, M. Teper and G. Schierholz, Phys. Lett. 116B (1982) 429 and Zeit. Phys. C 21 (1983) 167.
[91] V.A. Novikov et al., Nucl. Phys. B 237 (1984) 525.
[92] A. Billoire, R. Lacaze, A. Morel and H. Navelet, Phys. Lett. 80B (1979) 381.
[93] J.G. Körner, J.H. Kühn, M. Krammer and H. Schneider, Nucl. Phys. B 229 (1983) 115.
[94] K. Wilson, Phys. Rev. D 10 (1974) 2445;
J. Kogut, D. Sinclair and L. Susskind, Nucl. Phys. B 114 (1976) 199.
[95] R. Jaffe and K. Johnson, Phys. Lett. 60B (1976) 201.
J. Donoghue, K. Johnson and B.A. Li, Phys. Lett. 99B (1981) 416.
[96] M. Frank and P.J. O'Donnell, Phys. Lett. 144B (1984) 451 and Phys. Lett. 133B (1983) 253.
[97] S. Okubo, Phys. Lett. 5 (1963) 165;
G. Zweig, CERN-TH-401, 402 (1964);
J. Iizuka, Prog. Theor. Phys. Suppl. 37–38 (1966) 21.
[98] P.M. Fishbane and S. Meshkov, Comm. Nucl. Part. Sci. 13 (1984) 325.
[99] J.M. Cornwall and A. Soni, Phys. Rev. D 32 (1985) 764.

[100] W. Bartel et al., Phys. Lett. 66B (1977) 489.
[101] D.L. Scharre et al., SLAC-PUB-2321 (1979).
[102] J.D. Richman, PhD thesis, Caltech., CALT-68-1231 (1985).
[103] K.F. Einsweiler, PhD thesis, SLAC-278 (1984).
[104] G.W. Intemann Phys. Rev. D 27 (1983) 2755.
[105] H. Fritzsch and J.D. Jackson, Phys. Lett. 66B (1977) 365.
[106] V.A. Novikov, M.A. Shifman, A.I. Vainshtein and V.I. Zakharov, Nucl. Phys. B 165 (1980) 55.
[107] J.L. Rosner, Phys. Rev. D 27 (1983) 1101.
[108] D.L. Scharre et al., Phys. Lett. 97B (1980) 329.
[109] C. Edwards et al., Phys. Rev. Lett. 49 (1982) 259.
[110] C. Edwards et al., Phys. Rev. Lett. 51 (1983) 859.
[111] J.J. Becker, PhD thesis, Univ. of Illinois (1984).
[112] S. Berman and M. Jacob, Phys. Rev. B 139 (1965) 1023.
[113] R.J. Jaffe, Phys. Rev. D 15 (1977) 267, 281.
[114] M. Frank, N. Isgur, P.J. O'Donnell and J. Weinstein, Phys. Lett. 158B (1985) 442.
[115] W.F. Palmer and F. Pinsky, Phys. Rev. D 27 (1983) 2219.
[116] P. Baillon et al., Nuovo Cimento A 50 (1967) 393 and J. Phys. C 3 (1982) 86.
[117] C. Dionisi et al., Nucl. Phys. B 169 (1980) 1.
[118] T.A. Armstrong et al., Phys. Lett. 146B (1984) 273.
[119] S.U. Chung et al., Phys. Rev. Lett. 55 (1985) 779.
[120] A. Ando et al., contributed paper to the 1985 International Symposium on Lepton and Photon Inrteractions, Kyoto, KEK-preprint 85-15 (1985).
[121] S. Cooper, SLAC-PUB-3819 (1985).
[122] L. Montanet, Rep. Prog. Phys. 46 (1983) 337.
[123] M. Bander, B. Klima, U. Maor and D. Silverman, Phys. Lett. 134B (1984) 258.
[124] N.A. Törnqvist, Nucl. Phys. B 203 (1982) 268.
[125] Ph. Gavillet et al., Zeit. Phys. C 16 (1982) 119.
[126] N.R. Stanton et al., Phys. Rev. Lett. 42 (1979) 346.
[127] S. Ono and F. Schöberl, Phys. Lett. 118B (1982) 419.
[128] S. Ono, Phys. Rev. D 28 (1983) 558.
[129] J.M. Cornwall and A. Soni, Phys. Lett. 120B (1983) 431.
[130] K. Senba and M. Tanimoto, Phys. Lett. 106B (1981) 215.
[131] A. Lahiri and B. Bagchi, Phys. Lett. 112B (1982) 406.
[132] W.F. Palmer, S.S. Pinsky and C. Bender, Phys. Rev. D 30 (1984) 1002.
[133] K. Milton, W. Palmer and S. Pinsky, Proc. 17th Rencontre de Moriond, Les Arcs, France, 1982.
[134] J.F. Donoghue, Phys. Rev. D 30 (1984) 114.
[135] C. Edwards, PhD thesis, Caltech., CALT-68-1165 (1984).
[136] A. Bettini et al., Nuovo Cimento A 42 (1966) 695;
H. Braun et al., Nucl. Phys. B 30 (1971) 213.
[137] R. Brandelik et al., Phys. Lett. 97B (1980) 448;
D.L. Burke et al., Phys. Lett. 103B (1981) 153.
[138] H. Kolanoski, Two Photon Physics at e^+e^- Storage Rings, Springer Tracts In Modern Physics (1985).
[139] A. Etkin et al., Phys. Rev. Lett. 40 (1978) 422.
[140] S.J. Lindenbaum, Nuovo Cimento A 65 (1981) 222.
[141] D.L. Burke et al., Phys. Rev. Lett. 49 (1982) 632.
[142] R.M. Baltrusaitis et al., SLAC-PUB-3682, submitted to Phys. Rev. D.
[143] R.M. Baltrusaitis et al., Phys. Rev. Lett. 55 (1985) 1723.
[144] N. Wermes, Proc. 5th Int. Conf. Physics in Collision, Autun, France, 1985, and SLAC-PUB-3730 (1985).
[145] N.N. Achasov and G.N. Shestakov, Phys. Lett. 156B (1985) 434.
[146] G. Alexander et al., Phys. Lett. 72B (1978) 493;
G. Alexander et al., Phys. Lett. 76B (1978) 652.
[147] D.L. Scharre et al., SLAC-PUB-2321 (1979).
[148] C. Edwards et al., Phys. Rev. D 25 (1982) 3065.
[149] A. Devoto and W.W. Repko, Phys. Rev. D 27 (1983) 692.
[150] P.K. Kabir and A.J.G. Hey, Phys. Rev. D 13 (1976) 3161; note that the first occurrence of $\sin^2\theta_m$ in eq. (6) of this reference should be replaced by $\sin 2\theta_m$.
[151] F.E. Close, Phys. Rev. D 27 (1983) 311.
[152] B.A. Li and Q.X. Shen, Phys. Lett. 126B (1983) 125.

[153] A. Bramon, R. Casas, J. Casulleras and F. Cornet, Zeit. Phys. C 28 (1985) 573.
[154] M.E.B. Franklin, PhD thesis, SLAC-254 (1982).
[155] C. Edwards et al., Phys. Rev. Lett. 48 (1982) 458.
[156] F. Binon et al., Phys. Lett. 140B (1984) 264.
[157] J.F. Donoghue, International Europhysics Conference on High Energy Physics, Bari, 1985, and U. of Mass. UMHEP-235.
[158] M. Tanimoto, Phys. Lett. 116B (1982) 198;
A. Le Yaouarc et al., Zeit. Phys. C 28 (1985) 309.
[159] M. Chanowitz and S. Sharpe, Phys. Lett. 132B (1983) 413.
[160] H.J. Schnitzer, Nucl. Phys. B 207 (1982) 131;
J.L. Rosner and S.F. Tuan, Phys. Rev. D 27 (1983) 1544;
S. Ono and O. Pène, Zeit. Phys. C 21 (1983) 109.
[161] T.A. Armstrong et al., CERN-EP 85-179 (1985), Phys. Lett. 167B (1986) 133.
[162] K.F. Einsweiler, Proc. Int. Europhysics Conf. High Energy Physics, Brighton, 1983;
D. Hitlin, Proc. Int. Symp. Lepton and Photon Interactions, Cornell, 1983.
[163] R.M. Baltrusaitis et al., Phys. Rev. Lett. 56 (1986) 107.
[164] S. Godfrey, R. Kokoski andf N. Isgur, Phys. Lett. 141B (1984) 439.
[165] B.F.L. Ward, Phys. Rev. D 31 (1985) 2849.
[166] H.E. Haber and G.L. Kane, Phys. Lett. 135B (1984) 196.
[167] R.S. Willey, Phys. Rev. Lett. 52 (1984) 585.
[168] F. Wilczek, Phys. Rev. Lett. 39 (1977) 1304.
[169] S. Weinberg, Phys. Rev. Lett. 36 (1967) 294;
A.D. Linde, Phys. Lett. 70B (1977) 306.
[170] J.F. Donoghue and L.F. Li, Phys. Rev. D 19 (1979) 945;
H.E. Haber and G.L. Kane, Phys. Lett. 135B (1984) 196;
L. Lane, S. Meshkov and F. Wilczek, Phys. Rev. Lett. 53 (1984) 1718;
S. Glashow and M. Machacek, Phys. Lett. 145B (1984) 302;
H. Georgi, A. Manohar and G. Moore, Phys. Lett. 149B (1984) 234;
R.S. Willey, Phys. Rev. Lett. 52 (1984) 585.
[171] S. Behrends et al., Phys. Lett. 137B (1984) 277;
J. Lee-Franzini, CUSB Collaboration, Proc. Int. Conf. Physics in Collision, Autun, France, July 1985.
[172] S. Weinberg, Phys. Rev. Lett. 40 (1978) 223.
[173] R.D. Peccei and H.R. Quinn, Phys. Rev. Lett. 38 (1977) 1440 and Phys. Rev. D 16 (1977) 1791.
[174] H. Faissner et al., Phys. Lett. 103B (1981) 234.
[175] D.J. Bechis et al., Phys. Rev. Lett. 42 (1979) 1511;
J.L. Vuilleumir et al., Phys. Lett. 101B (1981) 341;
J. Frère et al., Phys. Lett. 103B (1981) 129;
M. Wise, Phys. Lett. 103B (1981) 121;
A. Zehnder, Phys. Lett. 104B (1981) 494.
[176] F. Wilczek, Phys. Rev. Lett. 40 (1978) 279.
[177] C. Edwards et al., Phys. Rev. Lett. 48 (1982) 903.
[178] F.C. Porter and K. Königsmann, Phys. Rev. D 25 (1982) 1993.
[179] M. Sievertz et al., Phys. Rev. D 26 (1982) 717;
M.S. Alam et al., Phys. Rev. D 27 (1983) 1665.
[180] M. Dine, W. Fischler and M. Srednicki, Phys. Lett. 104B (1981) 199;
M.B. Wise, H. Georgi and S.L. Glashow, Phys. Rev. Lett. 47 (1981) 402.
[181] M.E.B. Franklin et al., Phys. Rev. Lett. 51 (1983) 963.
[182] G. Karl and W. Roberts, Phys. Lett. 144B (1984) 263.
[183] W.S. Hou and A. Soni, Phys. Rev. Lett. 50 (1983) 569.